

# A REVIEW OF IRRADIATION EFFECTS ON LWR CORE INTERNAL MATERIALS - IASCC SUSCEPTIBILITY AND CRACK GROWTH RATES OF AUSTENITIC STAINLESS STEELS

O. K. Chopra<sup>1</sup> and A. S. Rao<sup>2</sup>

<sup>1</sup>Environmental Science Division  
Argonne National Laboratory  
Argonne, IL 60439

<sup>2</sup>Division of Engineering  
US Nuclear Regulatory Commission  
Washington, DC 20555

## Abstract

Austenitic stainless steels (SSs) are used extensively as structural alloys in the internal components of light water reactor (LWR) pressure vessels because of their relatively high strength, ductility, and fracture toughness. However, exposure to neutron irradiation for extended periods changes the microstructure (radiation hardening) and microchemistry (radiation-induced segregation) of these steels, and degrades their fracture properties. Irradiation-assisted stress corrosion cracking (IASCC) is another degradation process that affects LWR internal components exposed to neutron radiation. The existing data on irradiated austenitic SSs were reviewed to evaluate the effects of key parameters such as material composition, irradiation dose, and water chemistry on IASCC susceptibility and crack growth rates of these materials in LWR environments. The significance of microstructural and microchemistry changes in the material on IASCC susceptibility is also discussed. The results are used to determine (a) the threshold fluence for IASCC and (b) the disposition curves for cyclic and IASCC growth rates for irradiated SSs in LWR environments.

## 1. Introduction

A major concern regarding the structural and functional integrity of LWR core internal components is IASCC of structural materials (i.e., primarily austenitic SSs). Several incidents of IASCC have occurred since the mid-1970s in control blade handles and instrumentation tubes of boiling water reactors (BWRs), and since the 1990s, in BWR core shroud and pressurized water reactor (PWR) baffle bolts. As the name implies, IASCC is literally the irradiation-assisted enhancement of SCC susceptibility of materials. Neutron irradiation increases the IASCC susceptibility of austenitic SSs by changing the material microstructure due to radiation hardening and material microchemistry due to radiation-induced segregation (RIS) [1-4]. The susceptibility of austenitic SSs to IASCC has been investigated by conducting slow-strain-rate-tensile (SSRT), crack growth rate (CGR), and crack initiation tests on irradiated material in simulated LWR environments [5-13]. The factors that influence IASCC of austenitic SSs include neutron irradiation conditions such as neutron fluence, flux, and energy spectrum, cold work, material composition, corrosion potential, water purity, temperature, and loading conditions. The susceptibility of austenitic SSs to IASCC increases with neutron fluence, corrosion potential, and water conductivity.

Furthermore, radiolysis of water leads to its dissociation into various molecular, ionic, and radical reaction products that interact to form  $H_2O_2$ ,  $H_2$ , and  $O_2$ . In BWRs, these species increase the corrosion potential, which is known to increase the susceptibility of SSs to IASCC. However, the addition of  $H_2$  to the reactor water greatly reduces the effect of radiolysis by scavenging the radiolysis products [13]. Since PWR coolants typically contain 2 ppm  $H_2$  (30 cc/kg), radiolysis has no effect on the corrosion potential in PWRs.

Laboratory SSRT data on irradiated austenitic SSs have been used to identify a threshold fluence above which IASCC is significant in austenitic SSs in normal water chemistry (NWC) BWR environments [3,14-16]. Although a threshold fluence level of  $5 \times 10^{20} \text{ n/cm}^2$  ( $E > 1 \text{ MeV}$ )\* (0.75 dpa) has been proposed for austenitic SSs in NWC BWR environments, the results in Fig. 1 indicate that the intergranular (IG) cracking susceptibility in some commercial-purity SSs increases rapidly at fluence levels above about  $2 \times 10^{20} \text{ n/cm}^2$  (0.3 dpa) and in high-purity heats of SSs at even lower fluence levels.

Experimental data on Type 304 and 316 SSs irradiated up to  $4.0 \times 10^{21} \text{ n/cm}^2$  (6.0 dpa) show a beneficial effect of reducing the corrosion potential of the environment on IASCC susceptibility [16,17]. However, a low corrosion potential does not provide immunity to IASCC if the fluence is high enough; IGSCC has been observed in baffle bolts in PWRs. Threshold fluence for IASCC is higher under low-potential BWR hydrogen water chemistry (HWC) or PWR primary water chemistry. It also varies with material composition and thermo-mechanical treatment [16].

This paper presents an assessment of the susceptibility of austenitic SSs to IASCC. The existing data have been evaluated to establish the effects of material parameters (such as composition, thermo-mechanical treatment, microstructure, microchemistry, yield strength, and stacking fault energy) and environmental parameters (such as water chemistry, irradiation temperature, dose, and dose rate) on IASCC susceptibility. The results are used to determine (a) the threshold fluence for IASCC and (b) the disposition curves for cyclic and IASCC growth rates for irradiated SSs in LWR environments. A superposition model is used to represent the fatigue CGRs. The potential deficiencies or knowledge gaps in the existing experimental data on degradation of LWR core internal materials due to neutron irradiation are also discussed.

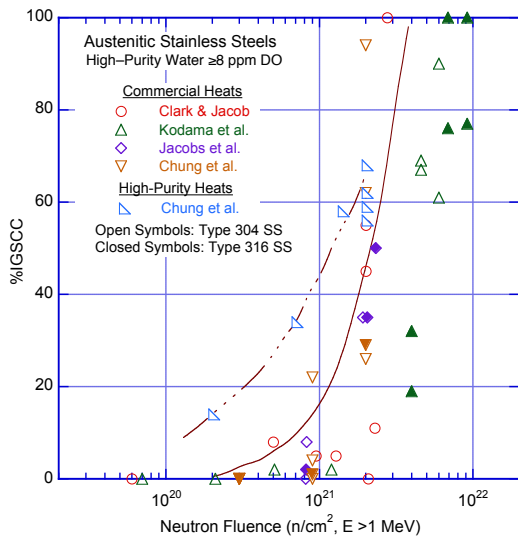


Fig. 1. Susceptibility of irradiated austenitic SSs to IGSCC as a function of fluence in high dissolved oxygen (DO) water.

\* All references to fluence levels are calculated for  $E \geq 1 \text{ MeV}$ .

## 2. IASCC susceptibility

It is well known that SCC of materials in high-temperature, high-pressure water depends on three factors: a susceptible material, relatively high stress, and aggressive environment. In the film rupture/slip oxidation model the fundamental elements of SCC have been described in terms of the processes that occur at the crack tip [18-20] and are considered to include: dynamic strain at the crack tip that disrupts the passive film thereby exposing fresh metal surface, followed by rapid metal oxidation and the subsequent repassivation a process that can be quantitatively linked to crack advance [14]. The kinetics of repassivation are primarily a function of the local chemistry and material composition; and the mass transport processes that establish the local crack tip chemistry [20]. The effect of water chemistry is particularly important because it can change the corrosion reactions at the crack tip. Metallurgical and microstructural parameters are also important because sensitization of the material by thermal treatment or irradiation hardening due to radiation damage can alter the localized deformation and creep processes at the crack tip, thereby changing the film rupture frequency.

A review of the existing data on IASCC susceptibility has identified the following key material and environmental parameters that influence the susceptibility of LWR core internal materials to IASCC.

### 2.1 Microstructure

Neutron irradiation of materials can produce damage by displacing atoms from their lattice position. Each displaced atom creates a vacancy and self-interstitial atom pair. These defects are unstable, and most of them are annihilated by recombination. The surviving defects rearrange into more stable configurations such as dislocation loops, network dislocations, precipitates, and cavities (or voids), or migrate to sinks such as grain boundaries or surfaces of second phase particles. The production, annihilation, and migration of the point defects lead to changes in the microstructure and microchemistry of the material. These changes vary with the material composition and thermo-mechanical treatment and irradiation temperature and dose rate [21]. Irradiation damage is characterized by either the neutron fluence ( $n/cm^2$ ) or the average number of displacements per atom (dpa).\*

Under LWR conditions, the microstructure produced by irradiation seems to change significantly for temperatures above 300°C. At 275-300°C, the defect structure primarily consists of small “black spot” defect clusters (<4 nm in diameter) and large dislocation loops (4-20 nm in diameter) that are primarily faulted interstitial Frank loops, whereas at higher temperatures the microstructure contains large faulted loops and network dislocations, and cavities/voids (clusters of vacancies and/or gas bubbles) and precipitates form at higher doses [21-26].

The size of the dislocation loops increases with increasing irradiation dose. The saturation size of the loops depends on the irradiation conditions and material characteristics. Under LWR conditions, the loop density saturates at a relatively low dose (about 1 dpa), and the average loop diameter saturates at about 5 dpa. Also, alloying elements can affect the material microstructure (e.g., P, Ti, and Nb increase the loop density and decrease loop size). The loop size increases and loop density decreases with irradiation temperature. At temperatures of 300-350°C, the microstructure primarily consists of large Frank loops and a network of tangled dislocations [21]. Also, cavities and voids form at high doses and high temperatures. Cavities or voids have not been observed in SSs irradiated below 300°C.

Irradiation at high temperatures leads to the formation of second phase particles. However, the available data suggest that radiation-induced precipitation is not a concern at temperatures below 350°C.

---

\* Conversion to dpa is as follows: for LWRs,  $E > 1$  MeV and  $10^{22}$   $n/cm^2 \approx 15$  dpa; and for fast reactors,  $E > 0.1$  MeV and  $10^{22}$   $n/cm^2 \approx 5$  dpa.

Metal carbides are the primary stable precipitates in 300-series SSs under LWR conditions, although RIS of Ni and Si to sinks may lead to the formation of  $\gamma'$  ( $\text{Ni}_3\text{Si}$ ) and G phase ( $\text{M}_6\text{Ni}_{16}\text{Si}_7$ ).

## 2.2 Microchemistry

Neutron irradiation also changes the microchemistry of the material due to RIS. The migration of vacancies and self-interstitial atoms to sinks, such as grain boundaries, dislocations, or precipitate surfaces, leads to local compositional changes. Elements such as Si, P, and Ni that are believed to migrate by interstitial mechanisms are enriched near regions that act as sinks for the point defects, while elements such as Cr, Mo, and Fe that exchange more rapidly with vacancies are depleted near sinks [2,3, 21]. The extent of segregation or depletion depends on the rate of generation and recombination of point defects (i.e., it depends on irradiation temperature and dose rate). Typically, RIS peaks at intermediate temperatures. It is reduced at low temperatures because of reduced mobility and at high temperatures due to back diffusion. Also, for a specific neutron dose, RIS is greater at lower dose rate. At 275-300°C, significant RIS is observed at irradiation doses as low as 0.1 to 5 dpa [2-21,26].

The radiation-induced changes in Cr and Si concentration at grain boundaries in several 300-series SSs irradiated in LWRs at 275-290°C are shown in Fig. 2 as a function of neutron dose. Most of the steels show a rapid decrease in Cr to about 13 wt.% and an increase in Si to about 4 wt.% at 5 dpa [26]. The data at dose levels above 10 dpa are limited, but they indicate that Cr content can decrease to 8-10 wt.% and Si content increase to 6 wt.% in 300-series SSs irradiated in LWRs at 300-320°C up to 65 dpa [26]. Under similar irradiation conditions, grain boundary Ni concentrations increase to about 22 wt.% at 5 dpa and can be as high as 30 wt.% at 65 dpa. The RIS behavior of minor elements such as P, S, C, N, and B, all of which segregate at the boundary, is not well established. These elements enrich grain boundaries but are difficult to measure.

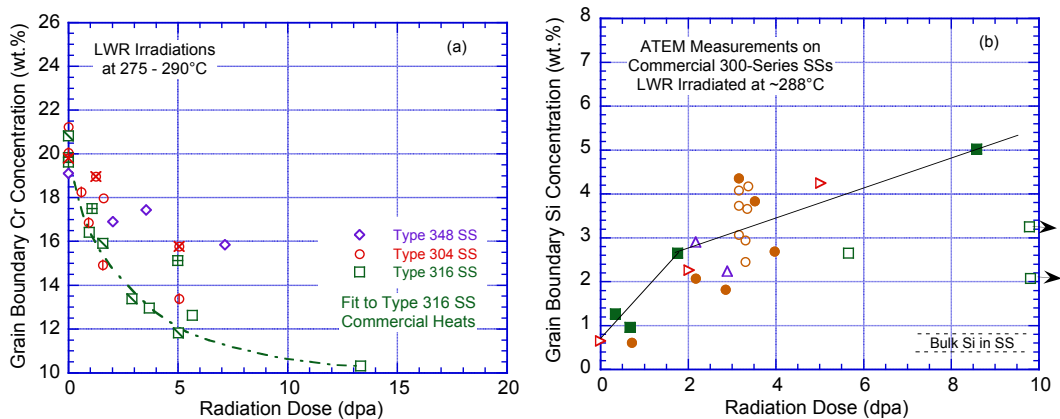


Fig. 2. (a) Cr and (b) Si concentration of grain boundary in irradiated stainless steels (Refs. 21,26).

## 2.3 Radiation hardening

The point defect clusters and precipitates produced by irradiation act, to varying extent, as obstacles to a dislocation motion, resulting in an increase in tensile strength and a reduction in ductility and fracture toughness of the material. In general, cavities (or voids) are strong barriers, large faulted Frank loops are intermediate barriers, and small loops and bubbles are weak barriers to dislocation motion [1]. The yield strength of irradiated SSs can increase up to five times that of the non-irradiated material after a neutron dose of about 5 dpa [4]. The influence of neutron fluence on the tensile properties of austenitic SSs is shown in Fig. 3 [12]. The yield and ultimate stresses increase and ductility decreases with irradiation.

At high neutron doses, as the irradiated yield strength approaches the ultimate strength of the material, there is a change in the deformation mode. Deformation by a planar slip mechanism is promoted, and the material exhibits strain softening [27]. This process is also termed “dislocation channeling,” whereby dislocation motion along a narrow band of slip planes clears the irradiation-induced defect structure, creating a defect-free channel that offers less resistance to subsequent dislocation motion or deformation. Nearly all SSs exhibit strain softening, and little or no uniform elongation, at irradiation dose above 3-5 dpa. The enhanced planar slip leads to a pronounced degradation in the fracture toughness of austenitic SSs. An assessment of neutron embrittlement of irradiated austenitic SSs is presented in a companion paper published elsewhere in this journal.

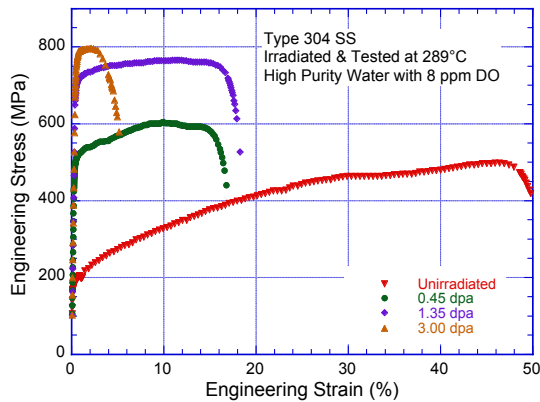


Fig. 3. The engineering stress-strain curves at 289°C for irradiated Type 304 SS (Ref. 12).

The extent of irradiation hardening and the increase in yield stress of austenitic SSs depend on the material composition and thermo-mechanical treatment, as well as the irradiation temperature. The greatest increase in yield strength for a given dose occurs at irradiation temperatures near 300°C (572°F). Studies on the effect of irradiation temperature on the yield strength and ductility of 20% cold-worked (CW) Type 316 SS irradiated in fast reactors [28] indicate that irradiation hardening and the loss of ductility are significantly more pronounced at 290°C (554°F), at least at low dose levels. Also, for a given neutron dose and irradiation temperature, the yield strength decreases with increasing test temperature. A similar trend is observed for SSs irradiated under LWR conditions.

#### 2.4 Yield strength

Three elements, in combination, influence IGSCC of austenitic SSs in BWR environments: a susceptible (sensitized) material, a significant tensile stress, and an aggressive environment. The NRC staff technical recommendations to reduce the susceptibility to IGSCC included the use of low carbon wrought austenitic SSs and weld metal, which are considered adequately resistant to sensitization by welding [29]. However, Andresen has shown that nonsensitized SSs are not immune to SCC; SSs with high yield strength (produced by cold work) are susceptible to IGSCC in ultra-high purity water [13]. The CGRs increase with increasing yield strength. Increases in yield strength can originate from surface or bulk cold work, weld shrinkage strain, precipitation hardening, oxide dispersion hardening, or even irradiation hardening; all of these increase SCC growth rates [30-32]. At a given yield strength, a similar susceptibility to cracking is observed in high- and low-potential environments; however, the CGRs in low potential water are an order of magnitude lower [13]. There is no significant difference among the different grades of SSs.

The effect of yield strength on SCC growth rates of LWR-irradiated austenitic SSs as a function of yield strength in NWC and HWC BWR environments at 289°C is shown in Fig. 4. In the NWC BWR

environment, CGRs in irradiated SSs increase rapidly for yield strength values in the range of about 200 to 800 MPa. At yield strengths of 700 MPa or lower, the growth rates are at least an order of magnitude lower in the HWC BWR environment. However, for 800 MPa or higher yield strengths (i.e., SSs irradiated above 3 dpa) the CGRs are comparable in both high- and low-potential environments.

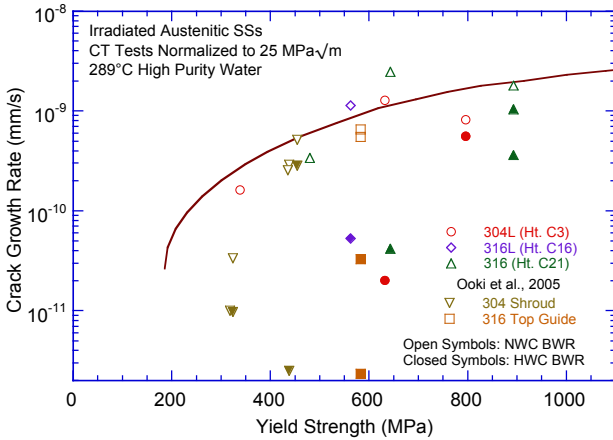


Fig. 4. Change in SCC growth rates at 289°C of LWR-irradiated austenitic stainless steels as a function of yield strength in NWC and HWC BWR environments (Refs. 30-32).

## 2.5 Silicon segregation

The increased susceptibility to IASCC and the loss of benefit of reducing potential in highly irradiated SSs have been attributed to the segregation of Si at the grain boundaries. The Si segregation is detrimental because at all relevant pH/potential conditions, Si oxidizes to  $\text{SiO}_2$ , which is highly soluble in hot water.

Unusually high SCC growth rates have been observed in CW SSs, containing 1.5 to 5 wt.% Si, in high-purity water with 2 ppm DO [33]. The CGR in 15% CW Type 304L SS with 5% Si (no Mo, Nb, or Ti additions) at 220°C (yield strength about 500 MPa) was  $2.2 \times 10^{-9}$  m/s at a stress intensity factor (K) of about  $30 \text{ MPa m}^{1/2}$ . The observed rate is a factor of 10 higher than the rates in most commercial SSs with similar levels of cold work/yield strength. More significant, the rate did not decrease when the environment was changed from high potential to low potential (95 ppb  $\text{H}_2$ ). In addition, decreasing K resulted in an initial decrease in CGR, from 2.2 to  $1 \times 10^{-9}$  m/s, but thereafter the CGR remained constant as the K decreased from 30 to  $15 \text{ MPa m}^{1/2}$  (Figs. 8 and 9 in Ref. 33).

In contrast to the increased susceptibility of high Si materials indicated by crack growth tests, SSRT test data on irradiated Type 304 and 316 SSs with 0.5-1.8 wt.% Si show the opposite behavior. For the same fluence level, steels with 1.5 to 1.8 wt.% Si showed less irradiation hardening and greater elongation than steels containing 0.5 wt.% Si [12]. Because most commercial SSs contain about 0.5% Si, its effect on irradiation hardening is not likely to be significant. Available data suggest that high concentrations of Si at grain boundaries due to RIS could increase susceptibility to IASCC. However, the absence of  $\gamma'$  silicide ( $\text{Ni}_3\text{Si}$ ) at the grain boundaries suggests that RIS of Ni and Si probably saturates at higher doses. The significance of Si segregation at grain boundaries on the SCC behavior of irradiated SSs is not clear, but Si segregation could be important. Crack growth tests should be conducted on irradiated material from commercial heats of SSs with similar compositions but different Si contents to establish the role of Si segregation on the IASCC susceptibility of irradiated SSs.

## 2.6 Stacking fault energy

The stacking fault energy (SFE) is an important parameter that determines the deformation mode. Alloys with Ni concentration >18 wt.% are highly resistant to IASCC compared to Type 304 SS with 8 wt.% Ni [4]. Alloys with low SFE, such as SSs with 8 wt.% Ni, deform entirely by planar slip, whereas there is no evidence of planar slip in alloys with high SFE (with >20 wt.% Ni). The increased susceptibility to IASCC is attributed to absorption of dislocations at the grain boundaries, which may cause grain boundary sliding ahead of the crack tip, resulting in crack extension and IASCC. Alternatively, progressively higher stresses at the grain boundary can change the film rupture frequency, thereby exposing bare metal surface and leading to oxidation/dissolution and crack extension. However, the role of the localized deformation mode on IASCC of austenitic SSs, as well as the possible contribution of SFE, should be further investigated.

## 2.7 LWR versus fast reactor irradiations

Because of the higher displacement rates, fast reactors are an attractive alternative for irradiating test materials to high dose ranges that cannot be achieved within a reasonable time in LWRs. However, the higher dose rates and differences in the thermal- and fast-neutron spectra may result in material microstructure and microchemistry that are not representative of LWR irradiations. Therefore, possible differences in material microstructure need to be examined.

Comparison of data on materials irradiated in fast reactors and LWRs indicates that the fast reactor irradiations may not be prototypic of LWRs, particularly at fluence levels above 5 dpa. The differences in the neutron spectrums could lead to higher defect survival rates in LWRs compared to fast reactors, whereas the differences in flux and temperature could lead to lower defect survival rates in LWRs compared to fast reactors. In addition to possible differences in RIS and radiation hardening, differences in helium generation, because helium can migrate to grain boundaries, could play an important role in IASCC of PWR core internals.

Studies on microstructural evolution in austenitic SSs indicate that at irradiation temperatures of 275-320°C, the Frank loop microstructure appears to be relatively insensitive to the displacement rates between LWRs and fast reactors [34]. The loop density in these steels irradiated either in LWRs or fast reactors is about  $2 \times 10^{23} \text{ m}^{-3}$ ; the saturation value was reached after about 2 dpa. However, there are some differences in the loop size of the irradiated steels. Also, additions of C, Si, P together and with other impurities appear to alter the evolution and type of microstructure of irradiated SSs in a complex way. The main difference between the LWR and fast reactor irradiations is the presence of He bubbles and cavities in materials irradiated to high dose levels in LWRs. Cavities are not observed in materials irradiated at similar temperatures in fast reactors. Also, He bubbles appear to form preferentially on the grain boundaries, which could lead to intergranular embrittlement of these materials [34].

The RIS of Cr, Ni, and Si in LWR- and BOR-60-irradiated austenitic SSs as a function of the neutron dose is shown in Fig. 5 [35]. In all cases, the data from fast reactor irradiation fall below the lower limit of the data from LWR irradiation (i.e., Cr depletion and Ni and Si enrichment are less in the fast reactor irradiated materials). These differences may influence the IASCC susceptibility or radiation embrittlement of these materials. The results indicate that the RIS in the fast reactor irradiated materials may not be representative of that observed under LWR irradiation conditions. Additional data on reactor core internals materials irradiated to doses above 10 dpa and at temperatures of 300-350°C under LWR conditions are needed to validate the applicability of the fast reactor data to LWRs.

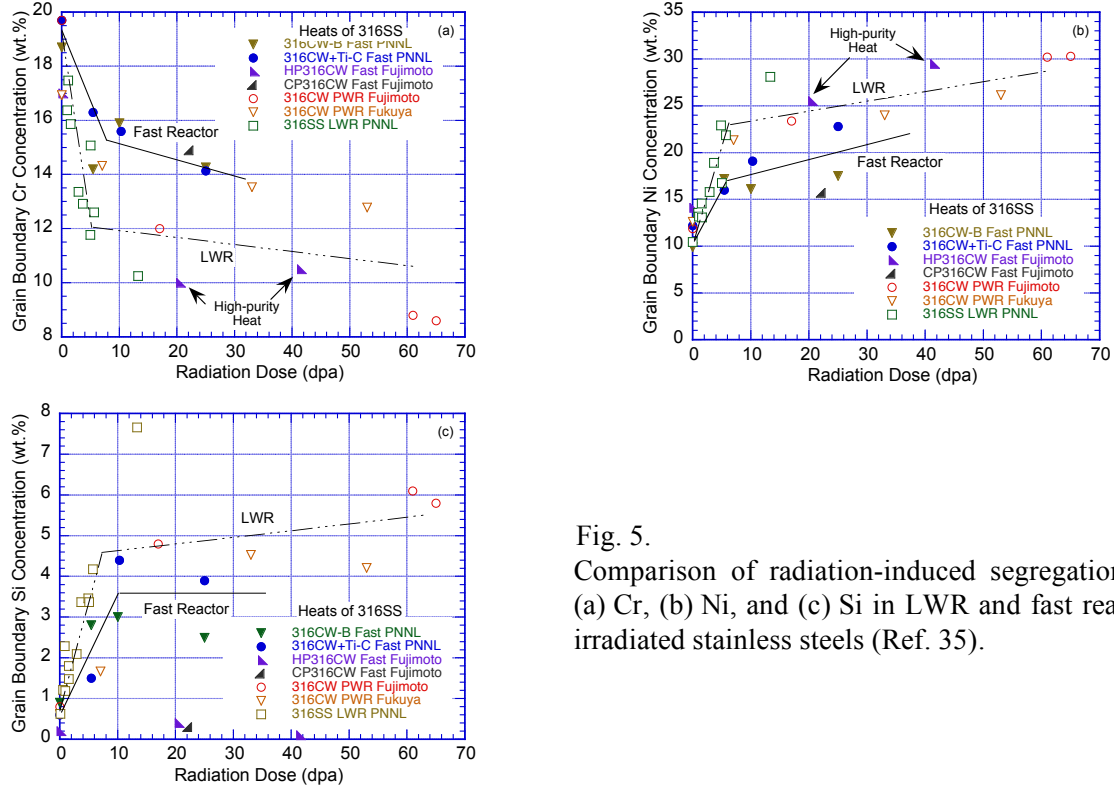


Fig. 5. Comparison of radiation-induced segregation of (a) Cr, (b) Ni, and (c) Si in LWR and fast reactor irradiated stainless steels (Ref. 35).

### 3. Tensile properties

Tensile properties data have been obtained on various grades of austenitic SSs, including weld HAZ material, weld metal, and CF-8 cast austenitic SSs, irradiated at temperatures of 300-400°C (572-752°F) in fast reactors and LWRs [36-40]. The 0.2% yield strength and total elongation of solution-annealed and CW SSs at elevated temperatures are plotted in Figs. 6 and 7 as a function of neutron dose. Most of the data in these figures were obtained on materials irradiated in the BOR-60 fast reactor. The curves in these figures represent the Materials Reliability Program (MRP)-developed correlations [41] for estimating the tensile properties as a function of neutron dose. The 0.2% yield strength, ultimate tensile strength, uniform elongation, and total elongation data at 330°C were fitted to an exponential equation of the form:

$$\text{Property} = A_0 + A_1 (1 - \exp(-d/d_0)), \quad (1)$$

where  $d$  is the neutron dose in dpa, and the coefficients  $A_0$ ,  $A_1$ , and  $d_0$  for the irradiated material property equations are listed in Tables 1 and 2.

Table 1. Material property equations for irradiated CW Type 316 stainless steel.

Property	Units	Property = $A_0 + A_1 (1 - \exp(-d/d_0))$		
		$A_0$	$A_1$	$d_0$
0.2% yield strength	MPa	500	470	3
Ultimate tensile strength	MPa	650	330	3
Uniform elongation	%	10	-9.7	2
Total elongation	%	18	-11	5

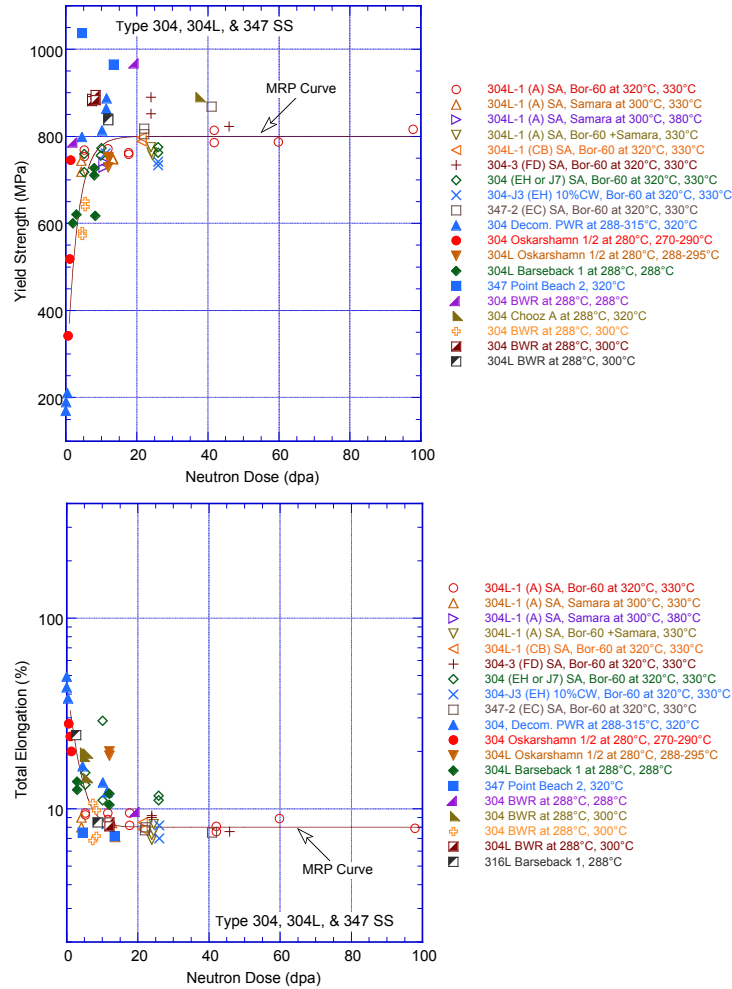


Fig. 6. Yield strength and total elongation as a function of neutron dose for solution-annealed Type 304, 304L, and 347 stainless steels at 270-380°C (Refs. 36-40).

Table 2. Material property equations for irradiated solution-annealed Type 304 stainless steel.

Property	Units	Property = $A_0 + A_1 (1 - \exp(-d/d_0))$		
		$A_0$	$A_1$	$d_0$
0.2% yield strength	MPa	200	600	3
Ultimate tensile strength	MPa	650	330	3
Uniform elongation	%	40	-39.5	1
Total elongation	%	45	-37	2.5

The results indicate that the tensile properties reach saturation at 5-20 dpa and do not change significantly at higher dose levels. The MRP correlations are primarily based on the fast reactor data and predict a saturated yield and ultimate strength value of 800 MPa for solution-annealed Type 304 SS and 970 and 980 MPa, respectively, for CW Type 316 SS. However, most of the data for yield and ultimate strength of LWR-irradiated materials are above the MRP curve [36-40]. Similarly, most of the data for uniform and total elongation of LWR-irradiated materials are below the MRP curve. Consequently, estimates of the tensile properties of irradiated austenitic SSs based on the MRP correlations would underestimate irradiation hardening and loss of ductility for LWR conditions. Additional data on austenitic SSs irradiated in LWRs to above 20 dpa are needed to better define the correlations for

estimating tensile properties of these materials under LWR operating conditions. The contribution of voids to irradiation hardening and loss of ductility should also be investigated.

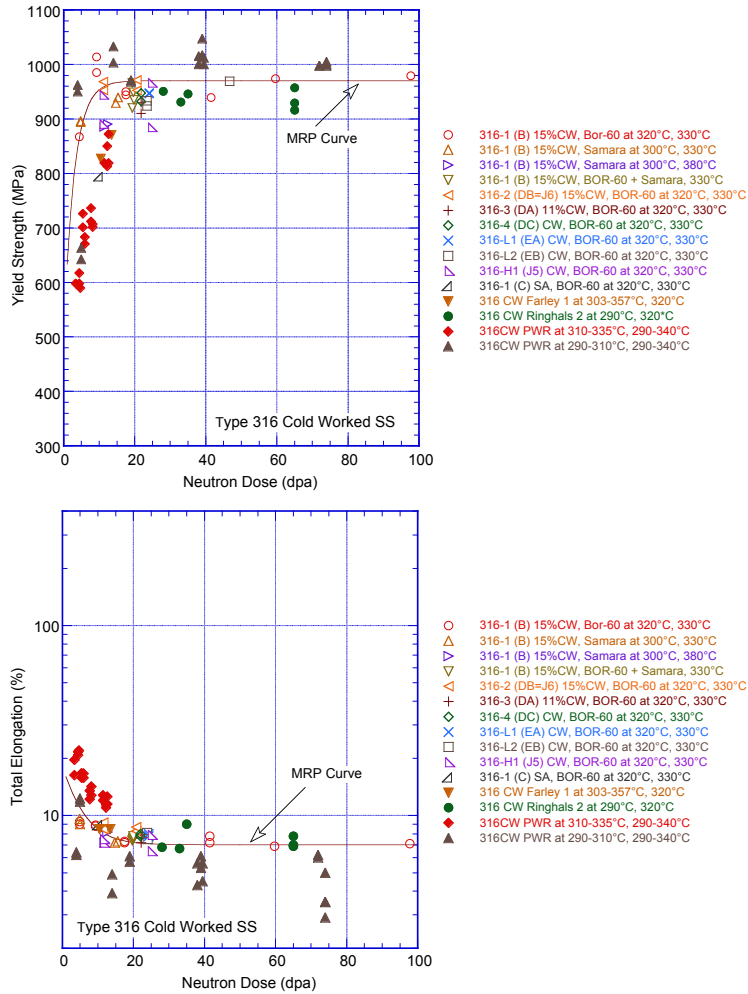


Fig. 7. Yield strength and total elongation as a function of neutron dose for cold-worked Type 316 stainless steels at 288-380°C (Refs. 36-40).

#### 4. SCC growth rates

Crack growth rate data have been obtained on irradiated wrought and cast austenitic SSs as well as SS weld metal and weld HAZ materials in LWR environments. The specimens were either machined from materials from LWR core internal components (mostly BWR components) or irradiated, after machining, under LWR irradiation conditions. However, some of the high neutron dose data have been obtained on materials irradiated in fast reactors, and the applicability of the data for estimating irradiation effects under LWR operating conditions needs to be evaluated.

Stress corrosion cracking is a complex phenomenon that is dependent on several parameters, such as material composition and processing, irradiation effects, water chemistry, loading condition, and temperature. As a result of these complexities and uncertainties in experimental measurements, the CGR vs. K data in LWR environments show significant variability (up to 1000X), and it is not yet possible to determine specific effects of these parameters on SCC growth rates with high confidence under all

conditions of interest. The quality of experimental CGR data and potential sources of uncertainty in experimental measurements and data scatter are discussed further in the following sections.

#### 4.1 Test procedures

Nearly all of the recent CGR data on irradiated materials in simulated BWR and PWR environments have been obtained on compact tension (CT) specimens (1/4-T or 1/2-T) or four-point bend specimens. The tests are performed in accordance with American Society for Testing and Materials (ASTM) methods. The specimens are fatigue pre-cracked (typically in air) to create a starter crack and actively loaded in the environment to determine the SCC growth rates and under cyclic loading to measure fatigue CGRs. The fatigue CGR tests are conducted with a triangular or slow/fast saw-tooth waveform with rise times up to 10,000 s and load ratio R between 0.2 and 0.9. The SCC growth rate tests are conducted under constant K with or without periodic partial unloading. The stress intensity factor for SCC tests (and maximum stress intensity factor  $K_{max}$  for fatigue tests) is in the range 3-40 MPa m<sup>1/2</sup>.

Also, the reversing direct-current (DC) potential difference method is used to monitor crack extension. The crack extensions determined from the DC potential drop method are corrected to match the final optically measured crack length. In most studies, crack lengths obtained from the DC potential drop method have shown good agreement with post-test fractographic measurements; typically, the potential drop measurements are 5-20% smaller. The CGRs are determined from the slope of the corrected crack length vs. time plots. For cyclic loading, the CGR can be expressed in terms of a time-based growth rate (da/dt) or a growth rate per cycle (da/dN).

The major source for variability in measured SCC growth rates is crack morphology. Typically, SCC of austenitic SSs in high-temperature water is intergranular (IG), whereas the starter crack for SCC tests is produced by fatigue cycling in air, which creates a transgranular (TG) crack. Depending on the susceptibility of the material to SCC, the TG crack may not transition to an IG crack during the test, or may transition only along a portion of the specimen width. Even if precracking is carried out in simulated LWR environments, an IG crack is not guaranteed. Under the more rapid cyclic loading, the crack growth is dominated by mechanical fatigue, which nearly always creates a TG crack. In some studies, the specimens are subsequently subjected to gentle cycling at relatively low frequency and high load ratio (to reduce the contribution of mechanical fatigue) and facilitate the transition of a TG crack to an IG crack [30,31]. The data scatter is significantly reduced in studies that follow such a test procedure.

#### 4.2 Specimen K/size criterion

The proposed K/size criterion for irradiated materials can also introduce inaccurate screening of the measured CGR data. Fracture mechanics is a correlative technology and does not attempt to describe the mechanisms that are occurring at the crack tip. It correlates the behavior of components with that of specimens through the use of the K parameter. If two cracks have the same K, then they have the same strains and stresses in a region near the crack tip. Mathematically, it can be shown that K characterizes the stresses and strains at the crack tip if the plastic zone size is "small enough". The ASTM specifications for specimen K/size criterion are intended to ensure that the plastic zone is small and K is controlling. For constant load tests, ASTM E 1681 requires that

$$B_{eff} \text{ and } (W - a) \geq 2.5 (K/\sigma_y)^2, \quad (2)$$

where W is the specimen width,  $\sigma_y$  is the yield stress of the material, a is crack length, and the  $B_{eff}$  is the specimen effective thickness, which is defined in terms of specimen thickness B and specimen net

thickness  $B_N$  as  $(B B_N)^{0.5}$ . For high strain-hardening materials [i.e., ratio of ultimate stress to yield stress  $(\sigma_u/\sigma_y) \geq 1.3$ ], Eq. 2 allows the use of the flow stress defined as  $\sigma_f = (\sigma_u + \sigma_y)/2$  rather than the yield stress.

This K/size criterion was developed for materials that show work hardening and, therefore, may not be applicable for materials irradiated to fluence levels where, on a local level, they do not strain harden and exhibit strain softening. An alternative K/size criterion based on an “effective yield stress” has been proposed where the irradiation-induced increase in yield stress is discounted by a factor of 2 for moderately irradiated materials [13], and by a factor of 3 for highly irradiated materials [42]. Thus, the effective yield stress is defined as  $\sigma_{\text{eff}} = (\sigma_{\text{yirr}} + \sigma_{\text{y nonirr}})/2$  or  $\sigma_{\text{eff}} = (\sigma_{\text{yirr}} + \sigma_{\text{y nonirr}})/3$ . These proposed criteria were not developed based on analyses of crack tip plastic strain or experimental comparisons of specimens with different degrees of constraint. Rather, they were proposed to explain some unusual IASCC growth rate results that did not show the benefit of decreased corrosion potential on growth rates in austenitic SSs irradiated to moderate irradiation levels (i.e., 3-4 dpa). The proposed criteria seem to be based on an implicit assumption that if the benefit of reduced corrosion potential on CGRs is effective at one K level and is not effective at a higher K level, then it must be due to a violation of the K/size criterion. The argument being that since austenitic SSs irradiated above approximately 3 dpa exhibit strain softening, K/size criterion based on the measured yield strength of the irradiated material is inadequate for such materials. It is not clear whether due consideration has been given to the possibility of other effects. Tensile property data for irradiated SSs indicate that strain softening in highly irradiated austenitic SSs is rarely more than 10-15%.

Recent investigations have evaluated the validity of the K/size criterion for irradiated materials by comparing the plastic strain distribution in a  $\frac{1}{2}$ -T CT specimen estimated from finite element method calculations with experimentally observed plastic deformation area [43,44]. The plastic zone size has been estimated to be 0.2-0.4 mm at  $K = 30 \text{ MPa m}^{1/2}$  [43]. The results indicate that for an austenitic SS irradiated to  $3 \times 10^{21} \text{ n/cm}^2$ , the appropriate K range for SCC growth rate tests is at least  $30 \text{ MPa m}^{1/2}$  for a (5.8-mm thick)  $\frac{1}{2}$ -T CT specimen. This is higher than that predicted by using the effective yield stress instead of the measured value. Detailed metallographic evaluation of the fracture surface also does not show any indication of a loss in constraint in these specimens (i.e., the fracture morphology does not change, and the fracture plane is straight and normal to the stress axis) [31]. In view of these studies, caution should be exercised to not use a K/size criterion that may screen out key experimental data.

#### 4.3 Rising K or $dK/da$ effects

In LWR components, K can increase as the crack depth, a, increases with crack advance, and it can increase and then decrease due to the through-wall weld residual stress profile, which is usually U-shaped. Consequently, as the crack advances through the wall, K can increase, remain relatively constant, or decrease, depending on the residual stress profile. Initially, when the crack depth is small, K could increase very rapidly because it is proportional to the square root of crack depth ( $K \propto \sigma\sqrt{a}$ ). Studies on austenitic SSs and Ni alloys in high-purity water with 2000 ppb  $\text{O}_2$  at  $288^\circ\text{C}$  have shown that rising K ( $+dK/da$ ) at K values that are relevant for LWR components can increase the CGRs significantly, whereas decreasing K ( $-dK/da$ ) has little or no effect [45]. Under rising K conditions, growth rates can be more than two orders of magnitude higher than those under constant K conditions.

As discussed by Andresen and Morra [45], dynamic strain at the crack tip is an important element of crack advance under SCC conditions. As the crack advances, the process of stress and strain redistribution sustains crack growth. It leads to slip offset, which ruptures the surface oxide film, and the crack advances due to oxidation/dissolution of the metal. Thus, there is an inherent synergy between

crack advance and growth rate itself (or  $dK/da$  as the crack advances). The data presented by Andresen and Morra [45] indicate that when changes in  $K$  are controlled by  $dK/da$ , very different responses can be seen for rising versus falling  $K$  conditions. For example, rising  $K$  results in an increased growth rate, which causes faster increase in  $K$ , which is a positive feedback. Decreasing  $K$  on the other hand yield negative feedback. These results indicate that CGR data obtained from tests where  $K$  was allowed to increase during the test or was decreased too fast may give erroneous results for the  $K$  dependence of SCC growth rates. Caution should be exercised while interpreting such results.

#### 4.4 Reloading effects

For some irradiated austenitic SS materials, small increases in the stress intensity factor  $K$  due to either load perturbations or the reloading portion of the partial unload/reload cycle during a SCC growth rate test result in a rapid or step-like crack extension [38]. The growth rates during such periods are as high as  $10^{-7}$  m/s. Such reloading effects produce a classic staircase appearance in the crack length vs. time plots. Similar behavior has been observed in nonirradiated CW SSs with high yield strength [19]. This behavior has often been attributed to the breaking of uncracked ligaments in the material and is believed to occur in materials with an uneven crack front. The significance and cause for this behavior should be investigated.

### 5. SCC growth rates

The effects of various material and environmental conditions on the SCC growth rates in austenitic SS materials irradiated in BWRs and PWRs are discussed next.

#### 5.1 BWR environments

*Dependence of stress intensity factor:* The SCC growth rates for various grades and heats of austenitic SSs irradiated from  $5 \times 10^{20}$  to  $2.5 \times 10^{22}$  n/cm<sup>2</sup> (0.75 to 37.5 dpa) in NWC BWR and HWC BWR environments are shown in Figs. 8a-c and Figs. 9a-c, respectively. These figures include data obtained for the crack growth rates of heat affected zone (HAZ) materials, both submerged arc weld (SAW) and shielded metal arc weld (SMAW), and for sensitized SSs. Also included are the  $K$  vs. CGR disposition curves proposed in the NRC report NUREG-0313 for nonirradiated sensitized austenitic SSs in high-purity water [29] and the curve proposed by EPRI for austenitic SS BWR core internal components [46]. The NUREG-0313 disposition curve is expressed as

$$da/dt \text{ (m/s)} = A1 (K)^{2.161}, \quad (3)$$

where  $K$  is in MPa m<sup>1/2</sup>, and the magnitude of  $A1$  depends on the water chemistry. The value of  $A1$  is  $2.1 \times 10^{-13}$  in water with 8 ppm DO and  $7.0 \times 10^{-14}$  in water with 0.2 ppm DO. It is smaller in low-potential HWC BWR and PWR primary water environments. The EPRI disposition curve for use in BWR core environments is expressed as

$$da/dt \text{ (m/s)} = A2 (K)^{2.5}, \quad (4)$$

where the constant  $A2$  is  $4.564 \times 10^{-13}$  in NWC BWR and  $1.512 \times 10^{-13}$  in HWC BWR environments. The EPRI correlations are based on two datasets; General Electric (GE) and Japan Power Engineering and Inspection Corp. (JAPEIC) data for SSs irradiated to 4.0-4.5 dpa [46], and the Halden reactor data (IFA 639 test series) for Type 304, 347, and 316NG SSs that were irradiated to 13.5, 2.25, and 1.35 dpa [47]. The significant results in NWC and HWC BWR environments are summarized as follows.



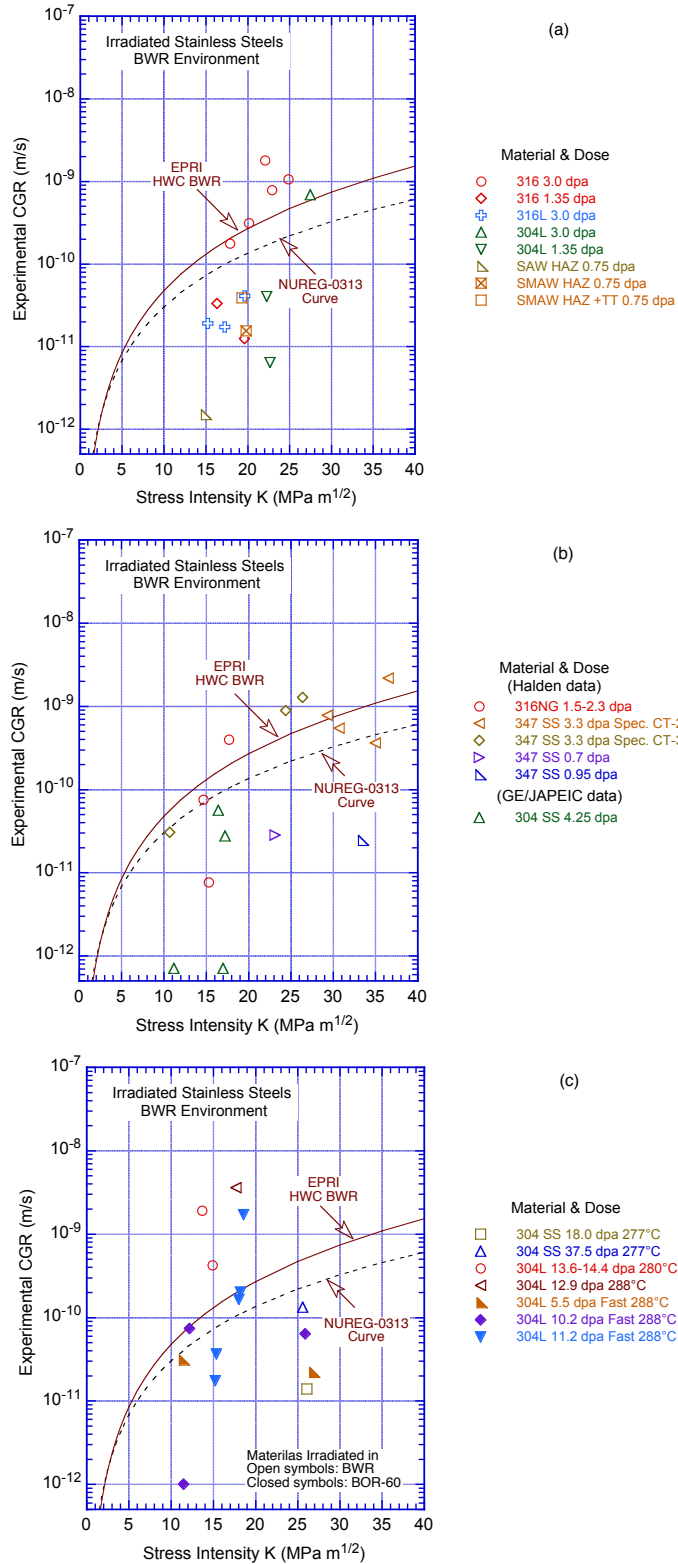


Fig. 9. SCC growth rates in HWC BWR environment on austenitic stainless steels irradiated to (a) 0.75-3.0 dpa (Refs. 30,31,51,52), (b) 0.7-4.25 dpa (Refs. 46-49), and (c) 5.5-37.5 dpa (Refs. 42,47-50).

In the NWC BWR environment, the SCC growth rates of austenitic SSs irradiated to 5 dpa could be a factor of 10 higher than the NUREG-0313 disposition curve for nonirradiated SSs in 8 ppm water, while austenitic SSs irradiated to 10-12 dpa could be a factor of 25 higher than the NUREG-0313 curve. For the end-of-60-year-life fluence level ( $3 \times 10^{21}$  n/cm<sup>2</sup> or 4.5 dpa), the CGRs of some SS materials could be significantly higher than the CGR disposition curve proposed by EPRI [46]. A CGR disposition curve that is a factor of 10 higher than the NUREG-0313 curve bounds nearly 80% of the data obtained in the NWC BWR environment for SSs irradiated up to 4.25 dpa. The results also indicate that the SCC growth rates for SSs irradiated in a PWR to 18 or 37.5 dpa are below the NUREG-0313 disposition curve for nonirradiated SSs. The reasons for the low CGRs observed for these highly irradiated materials are not clear. However, both materials came from the same reactor. It is possible that this behavior is unique to the material microstructure and microchemistry.

In general, CGR data obtained using test procedures in which the specimen was precracked in air and then transferred to the autoclave for the SCC test in the environment show much more variability at K values of 8-15 MPa m<sup>1/2</sup> (Halden data in Fig. 8) than data obtained using test procedures in which the specimen was precracked in the environment and the TG fatigue crack was transitioned to an IG crack by using slow fatigue cycling in the environment before starting the SCC test [see Argonne National Laboratory (ANL) and Studsvik data in Fig. 8]. This difference does not appear to be due to differences in material or irradiation conditions because data obtained at Halden and Studsvik on the same heat of Type 304L SS BWR control-rod blade material irradiated to comparable neutron dose [e.g., the two horizontal triangles ( $\triangleright$  and  $\triangleleft$ ) in Fig. 8c for Type 304L irradiated to 12.3 and 12.9 dpa, respectively] show more than a factor 10 higher growth rates for the material tested at Studsvik than for the material tested at Halden.

For the tests at ANL and Studsvik, the CGRs at 3-11 MPa m<sup>1/2</sup> were obtained by decreasing K from 14-20 MPa m<sup>1/2</sup> to the low values. As a result, the cracks were growing at a rate  $\geq 8 \times 10^{-10}$  m/s before K was decreased, whereas in the Halden data, tests were started at low K and the CGRs were  $< 1 \times 10^{-10}$  m/s.

The exponent for K, in Eq. 3, is typically between 1.7 and 2.7 for SSs irradiated up to about 5 dpa. For the Halden data, the exponent was about 2 for the IFA-639 test series and about 2.5 for the IFA-658 test series. Exponents are between 1.5 and 2.0 for the ANL data sets. For SSs irradiated to higher dose levels, this exponent could be as high as 7 for some data sets. However, for the SSs irradiated to 18.0 or 37.5 dpa, stable CGRs were observed only with periodic unloading, and the rates were relatively insensitive to changes in K.

The CGRs for the various grades and heats of SSs irradiated to the same dose level seem to be the same. For example, in the Halden study, the CGRs for Type 316NG and 347 SSs irradiated to 2.0-3.5 dpa are similar [47]. Similarly, in the ANL study, the CGRs of Type 304L, 316L, or 316 SSs irradiated to 1.35-3.0 dpa are comparable [31]. However, the rates for weld HAZ materials are slightly higher than those for solution-annealed materials (Fig. 8a). The higher rates most likely are due to weld residual strains, which could be as high as 30% of the room-temperature tensile strain [20].

*Effect of corrosion potential:* The data shown in Fig. 9 for SCC growth rates in the HWC BWR environment show a significant decrease in growth rates relative to those in the NWC BWR environment for SSs irradiated to less than 3 dpa; little or no reduction for some heats of SSs irradiated to 3-4 dpa; and no decrease for all SSs irradiated 12-14.5 dpa. Furthermore, the materials irradiated to 18 or 37.5 dpa did not show any benefit of decreased corrosion potential on CGRs, but they did not show a sustained crack advance under constant K. In these high dose materials, growth rates were established with periodic

unloading, and the rates even in NWC BWR environment were below the NUREG-0313 curve for nonirradiated SSs. However, as discussed above, the reason for these anomalous results is not known. Another significant feature of the cracking behavior of high dose materials was the “staircase” or reloading effect. In the HWC BWR environment, each unloading/reloading cycle was accompanied by a step or “jump” in crack length, creating a staircase or stepped crack growth. Although this behavior is often attributed to breaking of uncracked ligaments or straightening of the crack front, it is not clear why it should occur only in the HWC environment. Additional data in HWC BWR or PWR environments are needed on high-dose materials to better understand the IASCC behavior of austenitic SSs.

Some of the data for the 3-4 dpa materials (e.g., circles and triangle in Fig. 9a and diamonds and horizontal triangles in Fig. 9b) are often considered invalid because of the high K values that exceeded the proposed K/size criterion for irradiated materials (i.e., irradiation-induced increase in yield stress is discounted by a factor of 2). The arguments against the validity of the data do not seem to have a well-developed technical basis. The results in Fig. 9 indicate that the benefit of low-potential environments on SCC growth rates may be lost for some heats of SSs irradiated to fluence levels as low as 3 dpa. Some internal consistency checks can be used to demonstrate the validity of the Halden data for Type 347 SS irradiated to 2.3-3.3 dpa (diamonds in Figs. 8b and 9b). The growth rates observed during the test time from 720 to 840 h, for two identical specimens (CT-2 and CT-3) of this material tested in the HWC BWR environment, were  $7.32 \times 10^{-10}$  m/s at  $28.7 \text{ MPa m}^{1/2}$  and  $8.75 \times 10^{-10}$  m/s at  $23.6 \text{ MPa m}^{1/2}$ , respectively [47]. The environment was then changed to HWC, and the rates for the two specimens during test time 840 to 950 h were  $7.77 \times 10^{-10}$  m/s at  $29.3 \text{ MPa m}^{1/2}$  and  $8.9 \times 10^{-10}$  m/s at  $24.4 \text{ MPa m}^{1/2}$ , respectively. The growth rates for both specimens did not decrease after the corrosion potential was decreased. Also, note that the applied K for specimen CT-2 in NWC was higher than that for specimen CT-3 in HWC. If the measured CGR for specimen CT-3 is invalid in HWC, it should also be invalid for specimen CT-2 in NWC. The experimental data or the post-test fractography of these samples do not show any indication that the specimen constraints were exceeded for these specimens.

As discussed earlier, such results should not be screened out simply because they do not agree with the current understanding of the IASCC behavior of austenitic SSs. The feature that is common between specimens CT-2 and CT-3 is that although the K values are different, the growth rates for the specimens were comparable and may represent a threshold rate above which CGRs are relatively insensitive to changes in stress intensity factor K or corrosion potential. Additional data on SSs irradiated to 3-8 dpa are needed to accurately establish the threshold for IASCC susceptibility in low-potential PWR environments.

*Effect of Neutron Fluence:* The SCC growth rates for various grades and heats of austenitic SSs, irradiated from  $5 \times 10^{20}$  n/cm<sup>2</sup> to  $2.5 \times 10^{22}$  n/cm<sup>2</sup> (0.75 to 37.5 dpa) in NWC BWR and HWC BWR environments at 288°C and  $K = 20 \text{ MPa m}^{1/2}$  as a function of neutron dose, are shown in Figs. 10a and b, respectively. All materials except those irradiated in a fast reactor were irradiated in BWRs at temperatures of 280-300°C; the fast reactor irradiations were at 320°C. In the NWC BWR environment, the CGR increases above the NUREG-0313 level for doses >0.5 dpa, and the CGR also increases with dose out to about 10 dpa, although there is variability in the data. As noted previously, there are some anomalously data with low growth rates. In the HWC BWR environment, the CGRs do not exceed the NUREG-0313 levels until the fluence is  $\geq 3.0$  dpa. The CGRs for materials irradiated >5 dpa are comparable to those observed in the NWC BWR environment. The curves bound approximately 75<sup>th</sup> percentile of the data in the NWC environment and even more of the data for the HWC environment. The curves assume a threshold dose of 0.45 dpa and 2.7 dpa (or  $3 \times 10^{20}$  and  $1.8 \times 10^{21}$  n/cm<sup>2</sup>) in the NWC and HWC environment, respectively. The curves assume that constant A1 in the NUREG-0313 disposition curve (Eq. 3) varies with neutron dose. In the NWC environment A1 is taken as

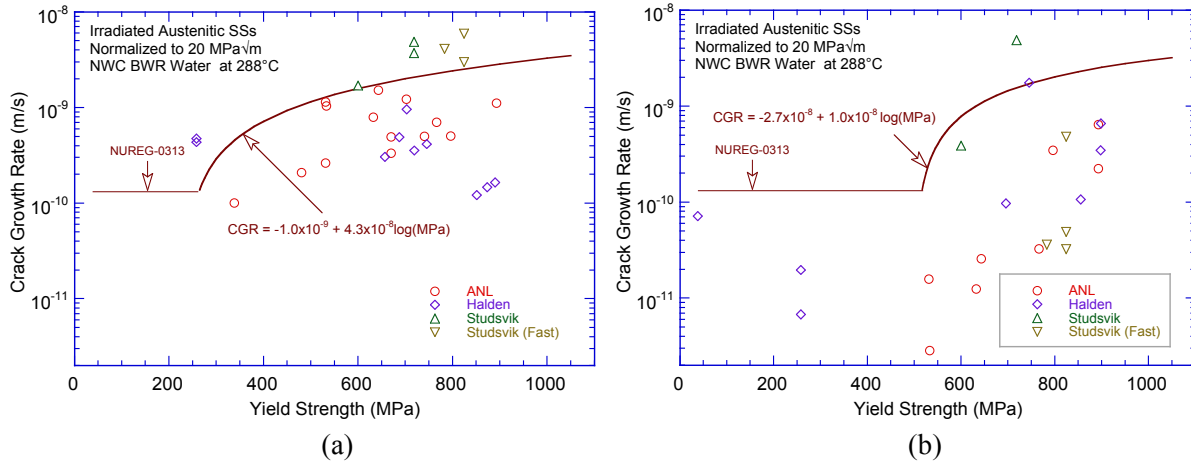


Fig. 10. SCC growth rates of irradiated austenitic stainless steels in (a) NWC and (b) HWC BWR environments at 288°C and  $K$  of 20 MPa  $m^{1/2}$  plotted as a function of neutron dose.

$$A1 = 1.21 \times 10^{-12} + 2.65 \times 10^{-12} \log(\text{dpa}), \quad (5)$$

and in the HWC environment as

$$A1 = 2.76 \times 10^{-12} + 6.82 \times 10^{-12} \log(\text{dpa}). \quad (6)$$

Note that because Eqs. 5 and 6 define the constant  $A1$  in Eq. 3, these values must be multiplied by  $(20)^{2.161}$  to obtain the expression for the CGR curves shown in Fig. 10.

### 5.2 PWR environment

Data on the SCC growth rate for irradiated austenitic SSs in the PWR environment have been obtained at Halden [38,53] on BWR irradiated materials, at Studsvik [50] on BOR-60 irradiated materials, and from EPRI sponsored studies on BWR and PWR irradiated materials. The total irradiation dose for these materials was in the range of 3.0-37.5 dpa with test temperatures of 288-340°C. The measured growth rates in various grades and heats of austenitic SSs in the PWR environment are shown in Fig. 11. There is a great deal of variability in the reported data. For a given material and irradiation condition, the variability is on the order of a factor of 10. The variability between materials and irradiation conditions is on the order of 1000.

Tests conducted on the same material at different temperatures indicate that the CGRs increase with increasing temperature. The temperature dependence of the SCC growth rates in irradiated and nonirradiated austenitic SSs yields activation energies between 60 and 150 kJ/mol. The CGRs of irradiated CW Type 316+Ti SS in the PWR environment at temperatures between 288 and 340°C yield an activation energy of 105 kJ/mol [50]. An activation energy of 100 kJ/mol was used to normalize the data shown in Fig. 11 to a temperature of 320°C; the normalized CGRs are shown in Fig. 12 for materials irradiated to (a) 3 dpa and (b) 11-25 dpa. The significant results are as follows.

In general, in the PWR environment at 320°C, the SCC growth rates of materials irradiated up to 12 dpa are above the EPRI disposition curve for the HWC BWR environment at 288°C. More than half the data points for Type 304L SS irradiated to 3 dpa are above the EPRI curve (Fig. 12a). The CGRs for Type 304L SS irradiated to 11.4 dpa and for fast-reactor-irradiated materials (except CW Type 316 SS) irradiated to 25 dpa are about two orders of magnitude higher than the NUREG-0313 curve (Fig 12b).

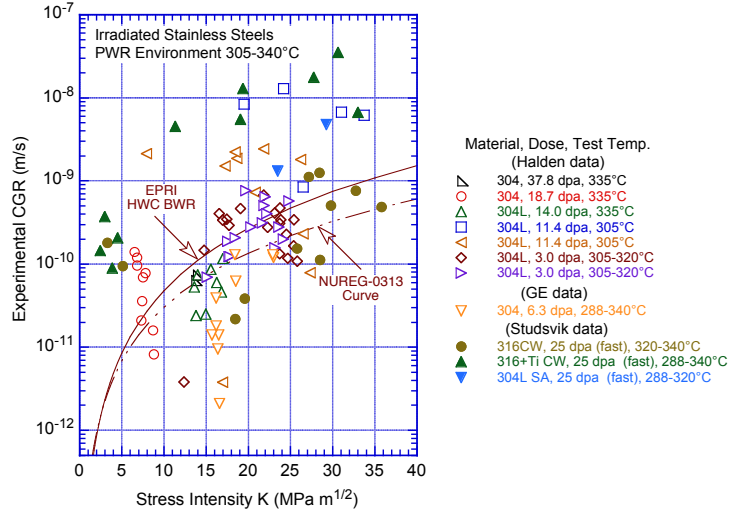


Fig. 11. SCC growth rates of austenitic stainless steels irradiated to 3.0-37.5 dpa in PWR environment (Refs. 38,50,53,54).

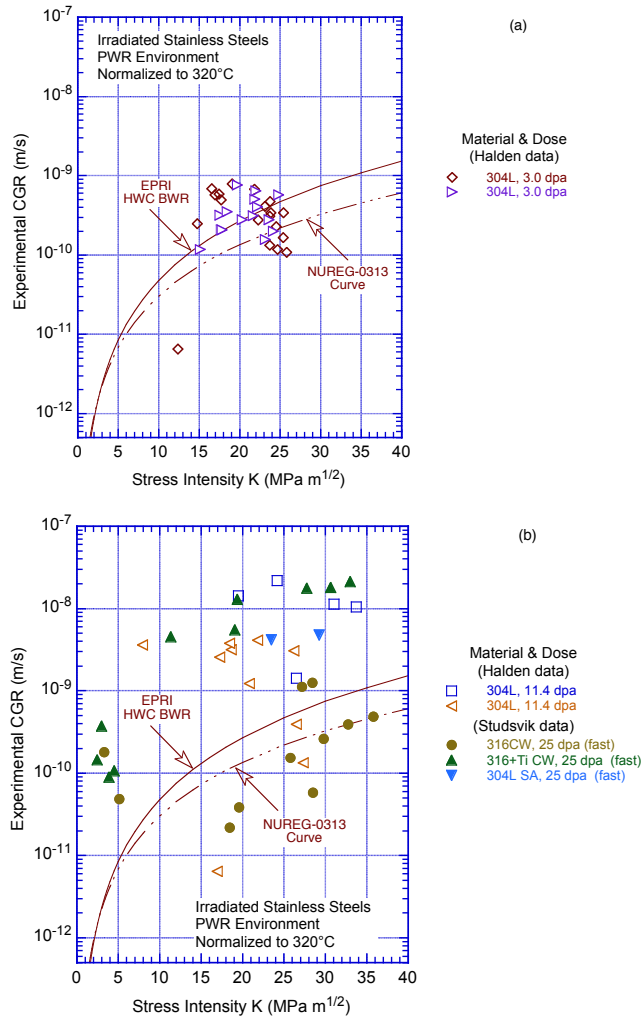


Fig. 12. Normalized SCC growth rates in PWR environment for austenitic stainless steels irradiated to (a) 3 dpa and (b) 11-25 dpa (Refs. 38,50,53,54).

The high growth rates in the 11.4 dpa material have been explained on the basis of possible effects of short test duration, high K values, and high grain-boundary Si concentration. As seen in Fig. 11 and observed earlier for the NWC BWR environment, CGRs in non-cold-worked SSs irradiated to 14 dpa or higher are mostly below the NUREG-0313 curve for nonirradiated SSs, and are not plotted in Fig. 12.

Figure 13 shows the SCC growth rates as a function of neutron dose for various grades and heats of austenitic SSs that had been irradiated to 0.7-37.5 dpa in HWC BWR water at 288°C or the PWR environment at 320°C, with  $K = 20 \text{ MPa m}^{1/2}$ . All materials except those irradiated in a fast reactor were irradiated in BWRs at temperatures of 280-300°C; the fast reactor irradiations were at 320°C. The data for the HWC BWR or PWR environments may be represented by the bounding curves shown in the figure. The curve represents a variation of A1 in the NUREG-0313 disposition curve (Eq. 3) with neutron dose that is expressed by Eq. 6.

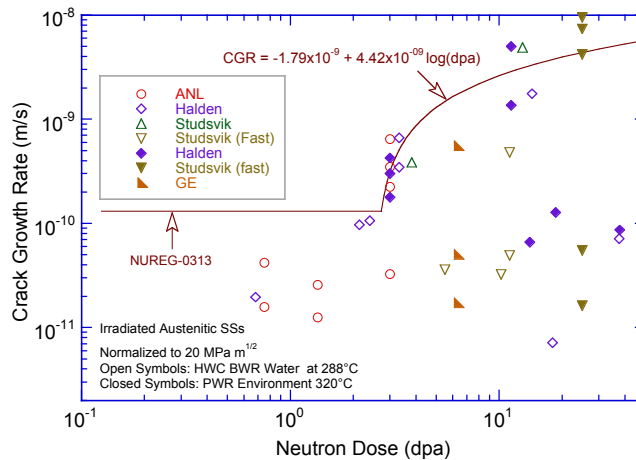


Fig. 13. Crack growth rates for irradiated austenitic stainless steels in HWC BWR water at 288°C or PWR environment at 320°C plotted as a function of neutron dose.

As noted previously, the available SCC growth rate data for irradiated austenitic SSs in PWR environments show significant variability. The reason for the high CGRs for some heats irradiated to 11.4 dpa and the unusually low growth rates in SSs irradiated above 18 dpa is not known. Also, most of the data in the PWR environment were obtained either on BWR irradiated material or materials irradiated in the BOR-60 fast reactor. The possible effects of differences in neutron spectrum and flux (fast vs. LWR) or irradiation temperature (288°C for BWRs vs. >320°C for PWRs) cannot be determined from the existing data. Additional data on PWR irradiated materials and materials irradiated at different temperatures (e.g., between 300 and 350°C) are needed to better understand the IASCC susceptibility of austenitic SSs in PWR environments.

## 6. Fatigue crack growth rates

Under cyclic loading, the time-based CGR,  $da/dt$ , (m/s) in an environment, can be expressed as the superposition of the rate in air and the rates due to corrosion fatigue and SCC, given as

$$(da/dt)_{env} = (da/dt)_{air} + (da/dt)_{cf} + (da/dt)_{scc}. \quad (7)$$

The  $CGR_{air}$  has been determined from the correlation developed by James and Jones [55]:

$$(da/dt)_{air} = C_{SS} S(R) \Delta K^{3.3}/t_r, \quad (8)$$

where  $\Delta K$  is in MPa m<sup>1/2</sup>, rise time  $t_r$  is in seconds, and the function  $S(R)$  is expressed in terms of the load ratio  $R$ :

$$\begin{aligned} S(R) &= 1.0 & R < 0 \\ S(R) &= 1.0 + 1.8R & 0 < R < 0.79 \\ S(R) &= -43.35 + 57.97R & 0.79 < R < 1.0. \end{aligned} \quad (9)$$

In Eq. 8,  $C_{SS}$  is expressed in terms of a third-order polynomial with temperature  $T$  (°C) [55]:

$$C_{SS} = 1.9142 \times 10^{-12} + 6.7911 \times 10^{-15} T - 1.6638 \times 10^{-17} T^2 + 3.9616 \times 10^{-20} T^3 \quad (10)$$

Shack and Kassner [56] have investigated the effects of LWR coolant environments on fatigue CGR of nonirradiated austenitic SSs. In the absence of any significant contribution of SCC to growth rate, the CGRs in water with  $\approx 0.2$  ppm DO were best represented by the expression

$$(da/dt)_{env} = (da/dt)_{air} + 4.5 \times 10^{-5} (da/dt)_{air}^{0.5}, \quad (11)$$

and in water with  $\approx 8$  ppm DO by the expression,

$$(da/dt)_{env} = (da/dt)_{air} + 1.5 \times 10^{-4} (da/dt)_{air}^{0.5}. \quad (12)$$

In Eq. 7, the SCC growth rates are represented by the NUREG-0313 [29] correlation shown in Eq. 3 for nonirradiated materials, and by six times the NUREG-0313 rate for irradiated materials (where constant  $A_1$  in Eq. 3 is  $1.26 \times 10^{-12}$ ). For fatigue loading, contributions from mechanical fatigue, and to some extent, from corrosion fatigue are always present for austenitic SSs and Ni alloys in LWR environments. The SCC contribution may not be significant for nonirradiated materials in low-potential HWC BWR or PWR environments.

The only data on the effect of neutron irradiation on fatigue crack crack growth have been obtained under the fast breeder reactor program. The data were obtained on austenitic SSs irradiated in fast reactors (primarily EBR-II) at temperatures of 370-450°C and tested at 427-593°C. For Type 304 and 316 SS irradiated at 405-410°C to  $1.2 \times 10^{22}$  n/cm<sup>2</sup> ( $E > 0.1$  MeV) (6.0 dpa), the CGRs at 427°C are up to a factor of 2 higher than those for nonirradiated material at  $\Delta K$  values less than 44 MPa m<sup>1/2</sup> (40 ksi in.<sup>1/2</sup>), and CGRs are comparable or lower at higher values of  $\Delta K$ s [57]. A similar behavior is observed for Type 316 weld [58]. Fatigue CGR data on Type 304 and 20% CW Type 316 SSs irradiated in EBR-II reactor at slightly higher temperatures, 455-477°C, to  $1.3$  and  $9.0 \times 10^{21}$  n/cm<sup>2</sup> ( $E > 0.1$  MeV) (0.65 and 4.5 dpa), showed no effects on growth rates at 427°C, and slightly lower growth rates at 538°C [59,60] Also, tests on Type 304 and 316 SS irradiated in a thermal reactor, Advanced Test Reactor (ATR), at 288°C to  $1.8 \times 10^{21}$  n/cm<sup>2</sup> ( $E > 0.1$  MeV) and tested at 427°C showed superior resistance to crack growth; crack growth rates were 25 to 50% lower than those for nonirradiated materials [61]. These results indicate no significant effect of irradiation of fatigue CGRs of austenitic SSs at these temperatures and  $K$  values.

Experimental data for fatigue CGRs of SS weld HAZ materials irradiated to  $\approx 2.16$  dpa in air are plotted in Fig. 14 as a function of CGRs predicted by the James and Jones expression [55] under the same loading conditions. The results indicate that the CGRs for irradiated weld HAZ material can be adequately represented by the correlations developed by James and Jones for nonirradiated SSs .

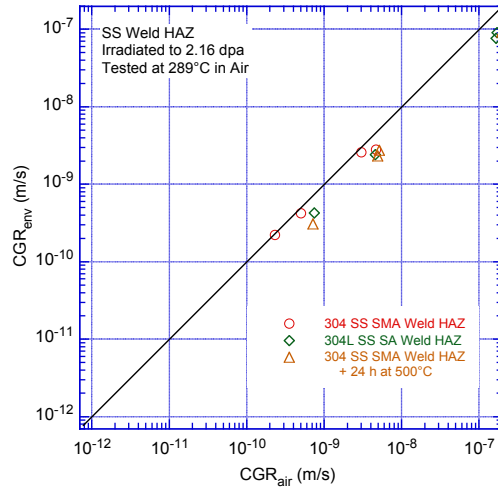


Fig. 14. Fatigue CGR data for irradiated SS in air (Ref. 31).

Under fatigue loading, experimental data for the CGR of solution-annealed Types 304 and 316 SSs irradiated up to 3 dpa and tested in high- and low-DO environments are plotted in Fig. 15 as a function of CGRs predicted in air for the same loading conditions [31]. In these figures, the data points that lie along the diagonal represent predominantly mechanical fatigue, and those that lie close to the model curve indicate environmentally enhanced crack growth. Austenitic SS irradiated to 0.45 dpa shows little environmental enhancement of CGRs in high-DO water. The curves in the figures are based on the superposition model (Eq. 7). For cyclic loading using either a triangular or a slow/fast sawtooth waveform,  $(da/dt)_{SCC}$  is determined by considering the contribution of SCC during the slow rise time of the cycle; an equivalent K is computed to determine the contribution of SCC. The calculated values of K are given in the figure.

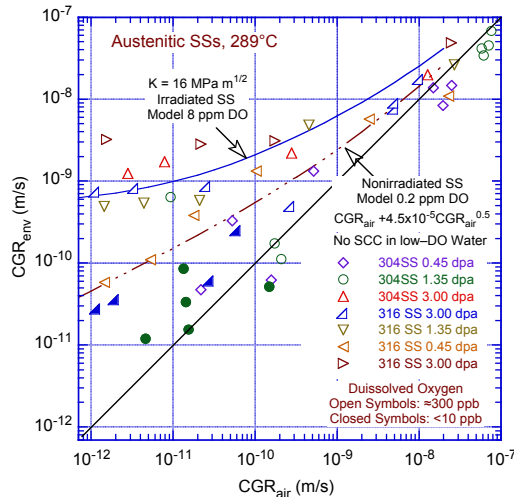


Fig. 15. Fatigue CGR for irradiated specimens of austenitic SSs at 289°C in high-purity water (Refs. 30,31).

The results for SSs irradiated to 1.35 or 3.0 dpa indicate significant enhancement of the CGRs in high-DO water under cyclic loading with long rise times. For austenitic SSs irradiated to 0.75-3.0 dpa,

the fatigue CGRs in water with  $\approx 300$  ppb DO may be represented by superposition of the SCC growth rates expressed as six times the NUREG-0313 curve and by the Shack/Kassner corrosion fatigue model for nonirradiated SSs in high-purity water with 8 ppm DO [56].

For continuous cyclic loading, decreasing the DO level has a beneficial effect on the CGRs of irradiated SSs; for example, decreasing the DO from  $\approx 300$  ppb DO to  $<30$  ppb DO lowers the CGR by a factor of 25 (closed symbols in Fig. 15). At 289°C, the fatigue CGRs for irradiated austenitic SSs in water with  $<30$  ppb DO are lower than those predicted by the Shack/Kassner model [56] for nonirradiated austenitic SSs in high-purity water with 0.2 ppm DO; there is no contribution of SCC in low-DO water.

Experimental data for CGRs of irradiated Type 304L SAW HAZ from the Grand Gulf core shroud and laboratory-prepared Type 304 SMAW HAZ in high-DO water are plotted as a function of those predicted in air for the same loading conditions in Fig. 16. The curves in the figures are based on the superposition model (Eq. 7). The results indicate significant environmental enhancement of CGRs for HAZ materials irradiated to 0.75 or 2.16 dpa. The CGRs of the Type 304L SAW HAZ are slightly lower than those of the Type 304 SMAW HAZ. The fatigue CGRs of SS weld HAZ materials irradiated to 0.75-2.16 dpa in water containing  $\approx 500$  ppb DO can be represented by superposition of the SCC growth rates for irradiated SSs (i.e., six times the NUREG-0313 curve) and the Shack/Kassner corrosion fatigue model for nonirradiated austenitic SSs in high-purity water with 8 ppm DO [56].

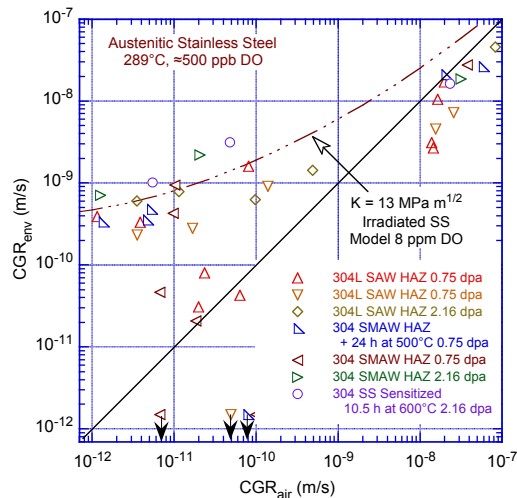


Fig. 16. Fatigue CGR for irradiated Type 304L SAW HAZ from the Grand Gulf core shroud and laboratory-prepared Type 304 SMAW HAZ in high-purity water at 289°C (Ref. 31).

## 7. Initiation of irradiated-assisted stress corrosion cracking

As discussed earlier, IASCC is an irradiation-induced increase in susceptibility of materials to SCC with increasing neutron fluence. The SCC of materials in high-temperature, high-pressure water depends on material susceptibility, high stresses, and an aggressive environment. However, the mechanism of IASCC in the PWR environment and the individual effect of various material and environmental parameters on IASCC are still not well understood. Although the degradation of tensile and fracture properties of austenitic SSs appears to saturate at 5-20 dpa, the susceptibility of SSs to IASCC continues to increase with neutron fluence. Both solution-annealed and CW austenitic SSs are susceptible to cracking in the PWR environment, but there is significant heat-to-heat variability. In general, the irradiation-induced degradation of fracture properties of austenitic SSs is slower in CW than solution-annealed materials because the CW materials have a high dislocation density, which slows irradiation

hardening and damage and suppresses void nucleation and swelling. However, at high neutron fluence levels (i.e., above 10-20 dpa or  $6.7 \times 10^{21}$  n/cm<sup>2</sup> to  $1.3 \times 10^{22}$  n/cm<sup>2</sup>, E>1.0 MeV), there is little or no difference in IASCC susceptibility of these materials in PWR environments.

For all wrought and cast austenitic SSs and their welds there does appear to be a threshold value of neutron fluence below which the materials can be considered not susceptible to IASCC in a PWR environment. Current estimates of a threshold value have been based on laboratory SSRT data. The following values have been proposed: a conservative threshold fluence of approximately  $6.7 \times 10^{20}$  n/cm<sup>2</sup> (1 dpa) [62], which represents the fluence at which IASCC can occur in a material after extremely high strains, and a more realistic value of  $2 \times 10^{21}$  n/cm<sup>2</sup> (3 dpa) [62,63], which represents the fluence at which IASCC can be initiated at above the yield stress of the material. For materials irradiated above this threshold, IASCC initiation data have also been used to define, for a given neutron dose, an apparent stress threshold below which IASCC initiation will not occur in a PWR environment. The SCC initiation data are obtained by conducting constant-load SCC initiation tests in a simulated PWR environment on O-ring, C-ring, or tensile specimens of irradiated materials [39,40,64-66]. The specimens are tested as a function of fluence and applied stress.

The constant-load IASCC initiation results plotted as stress (as percent of irradiated yield stress) versus time are shown in Fig. 17. The open symbols represent specimens that did not fail, and the closed symbols represent failed specimens. The same data are plotted as a function of neutron dose in Fig. 18. The results indicate that under a high enough stress, crack initiation in highly irradiated materials can occur quite rapidly (i.e., within 500 h). Furthermore, 80% of these failures (closed symbols) occurred within 150 h. The results also indicate a stress threshold below which cracks did not initiate even after several thousands of hours. Data on CW Type 316 SS irradiated in commercial PWRs show that at 26 dpa cracks initiated at stresses above approximately 62% of the irradiated yield stress [64]. In Fig. 18, for SSs irradiated to very high fluence levels, the stress threshold has been defined as 50% of irradiated yield stress, although two data points (closed inverted triangles) fall below this threshold. The stress threshold is shown as dash-dot line in Fig. 17. The IASCC initiation data also indicate significant scatter with respect to failure vs. non-failure, and the time to failure. For example, in a set of six identical specimens simultaneously tested, four failed and two did not. Also, of the four specimens that did fail, time to failure varied from 29 to 483 h. Therefore, sufficiently large numbers of specimens have to be

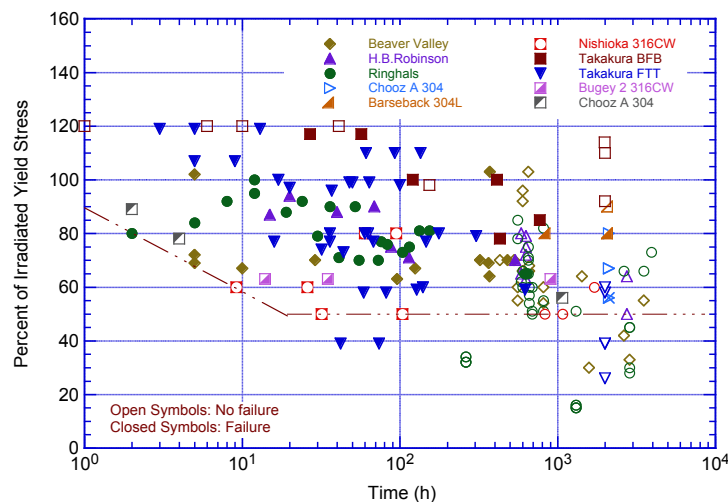


Fig. 17. Stress as percent of irradiated yield stress vs. time data for IASCC flaw initiation in austenitic stainless steels in a PWR environment (Refs. 39,40,62-66).

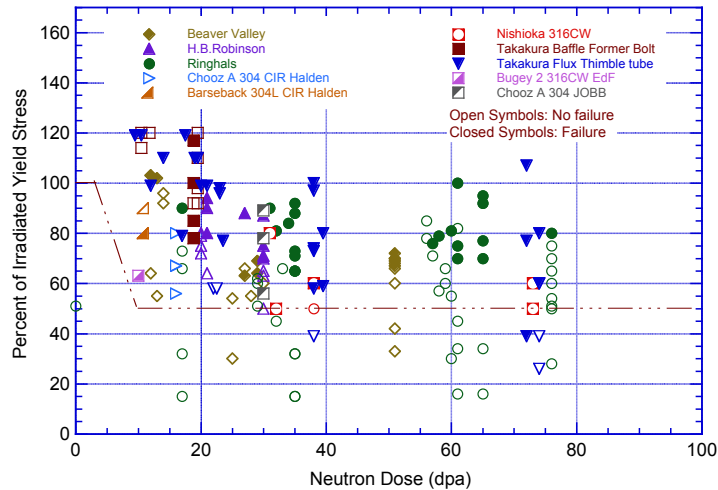


Fig. 18. Stress as percent of irradiated yield stress vs. neutron dose for IASCC flow initiation in austenitic stainless steels in a PWR environment (Refs. 39,40,62-66).

tested to identify valid data trends.

The IASCC initiation data have been used to estimate, for a given neutron dose, a lower bound stress vs. time-to-failure curve for austenitic SSs irradiated to 71-76 dpa. The curve in Fig. 19 represents for a specific irradiated material, the shortest time to initiate IASCC at a given stress in the PWR environment. These curves are extrapolated to 40-y or 60-y reactor life [i.e., 32- or 48-y effective full power year (EFPY)] to define an apparent stress threshold below which IASCC initiation will not occur for that material within a specified time, say, the reactor lifetime. Such results are used to develop the curves for stress vs. neutron fluence threshold that predict time for IASCC initiation as a function of stress and fluence.

Figure 20 presents two curves that define the approximate stress and neutron fluence for IASCC initiation in a relatively short time (i.e., 100 h) and after a very long time. The latter may be used as the lower bound for stress and fluence below which IASCC is not likely to occur within the lifetime of the reactor. However, the data that were used to develop these curves do not account for the effect of

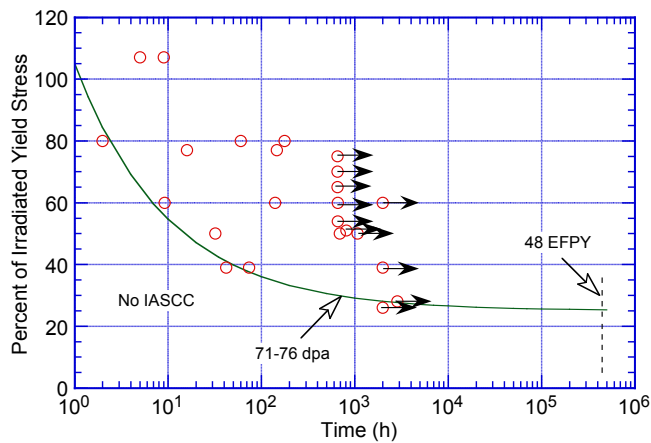


Fig. 19. Percent of irradiated yield stress vs. time for IASCC flow initiation in austenitic stainless steel irradiated to 71-76 dpa in PWR environment (Refs. 40,64,65).

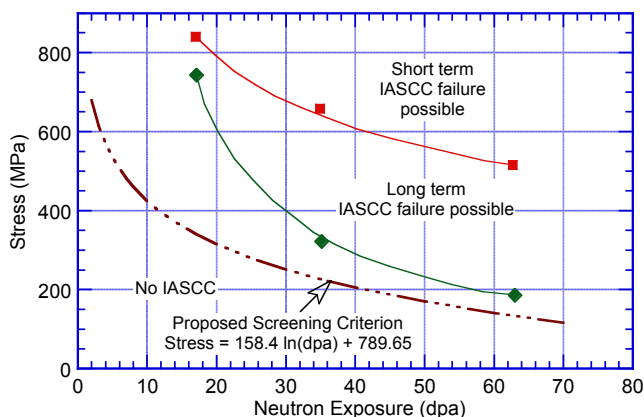


Fig. 20. Time for initiation of IASCC in irradiated austenitic stainless steels as a function of stress (Refs. 39,62).

material composition, material variability between heats, or the differences between solution-annealed or CW material. To account for material variability and uncertainty due to data scatter, MRP has proposed a screening curve, shown in Fig. 20, for IASCC initiation of austenitic SSs. This curve is used to divide various PWR core internal components into different categories of aging management strategies during the initial screening process.

Such an approach for defining neutron dose/applied stress thresholds for austenitic SSs is limited by the adequacy of the database used for developing the screening curve. First of all, insufficient data are currently available to adequately define an IASCC initiation curve correlating stress and neutron fluence. Considerably more data are needed to account for uncertainties due to data scatter, material variability, irradiation temperature, neutron spectrum effects, and water chemistry. As more information has been added to the IASCC initiation database, the threshold stress below which IASCC is considered not likely to occur during a 60-y reactor lifetime has been decreased from an initial value of 62% to 50% and now possibly 40% of the irradiated yield stress. Although a threshold fluence of 3 dpa has been defined for IASCC in the PWR environment, there are no IASCC initiation data on austenitic SSs irradiated between 3 and 9.5 dpa. Thus, in Fig. 18, for materials irradiated to 3-10 dpa, the threshold stress for IASCC initiation is defined arbitrarily by a straight line between 3 and 10 dpa. In addition, the existing database for IASCC initiation does not consider the effects of the following parameters that are known to influence IASCC susceptibility:

*Material type, composition, and condition:* The available IASCC initiation data have been obtained primarily on CW Type 316 SS, and data on solution-annealed Type 304, 304L, or 316 SS are limited. Also, there are no data on cast austenitic SSs, SS welds, and weld HAZ materials. Additional IASCC initiation data should be obtained on these materials irradiated to neutron fluence levels relevant for PWR core internals. Also, the increased susceptibility to IASCC and the loss of benefit of reduced corrosion potential on IASCC susceptibility in highly irradiated SSs are often attributed to the segregation of Si at the grain boundaries. Initiation data should be obtained on irradiated material from commercial heats of SSs with similar compositions but different Si contents to establish the role of Si segregation on the IASCC susceptibility of irradiated SSs.

*Irradiation temperature:* Nearly all of the high fluence (above 20 dpa) data and the majority of the low fluence data on IASCC initiation have been obtained on materials irradiated below 325°C. Consequently, the database does not include the potential effects of additional precipitate phases, voids,

and cavities, which are observed in SSs irradiated to high fluence levels at temperatures above 320°C. Also, He bubbles have been observed in SSs irradiated in reactors with high thermal neutron fluxes, and could also influence IASCC initiation.

*Neutron spectrum:* The current IASCC initiation data include some tests on austenitic SS irradiated in the BOR-60 fast reactor. Several studies have shown that materials irradiated in fast reactors exhibit lower susceptibility to IASCC than those irradiated in LWRs. Such data are not included in Figs. 17 and 18. Caution should be exercised when using fast reactor data to assess the degradation of LWR core internal materials.

*Water chemistry:* The addition of H<sub>2</sub> to the reactor water greatly reduces the effect of radiolysis by scavenging the radiolysis products. Because PWR coolants typically contain 2 ppm H<sub>2</sub> (30 cc/kg), radiolysis has no effect on the corrosion potential in PWRs. However, in reactor core internal components, IASCC is likely to occur under creviced conditions (i.e., under off-normal water chemistry). Nearly all of the IASCC initiation tests have been conducted in the normal PWR environment, and the possible effects of impurities on initiation have not been investigated.

## 8. Summary

The existing data have been reviewed to identify the key material parameters (such as composition, thermo-mechanical treatment, microstructure, microchemistry, yield strength, and stacking fault energy) and environmental parameters (such as water chemistry, irradiation temperature, dose, and dose rate) that influence IASCC, and to establish their effects on IASCC susceptibility of austenitic SSs.

The microstructural changes in austenitic SSs due to neutron irradiation vary with the material composition, irradiation temperature, and neutron fluence, flux, and energy spectrum. At 275-300°C, the loop density saturates at about 1 dpa, and the average loop diameter saturates at 5 dpa. In general, the loop size increases and loop density decreases with irradiation temperature. Irradiation temperatures above 350°C lead to the formation of second phase particles. Cavities and voids form at high doses and high temperatures. Under LWR conditions, metal carbides are the primary stable precipitates in 300-series SSs, although RIS of Ni and Si to sinks may lead to the formation of  $\gamma'$  phase (Ni<sub>3</sub>Si) and G phase (M<sub>6</sub>Ni<sub>16</sub>Si<sub>7</sub>). The microchemistry of the material is also changed due to RIS; Si, P, and Ni are enriched at regions such as grain boundaries, while Cr, Mo, and Fe are depleted. The extent of RIS depends on irradiation temperature and dose rate. At LWR temperatures, significant segregation is observed at an irradiation dose of 0.1 dpa, and the effect either saturates or changes very slowly beyond 5 dpa.

Most of the studies on microstructural characterization have been conducted on BWR-irradiated materials, and studies on PWR-irradiated materials (above 320°C) are limited. Additional microstructural data, including the distribution of voids/cavities and second phase particles, should be obtained on austenitic SSs irradiated in PWRs above 10 dpa and at temperatures above 300°C. Also, the redistribution of S, P, C, N, and B in SSs irradiated above 15 dpa needs to be investigated to establish its significance on the IASCC susceptibility of SSs.

The yield strength of irradiated SSs can increase up to five times that of the nonirradiated material after a neutron dose of about 5 dpa. For austenitic SSs, the greatest increase in yield strength for a given irradiation level occurs at irradiation temperatures near 300°C (572°F). The change in yield strength correlates well with the changes in dislocation structure of the material; the yield strength also either saturates or increases very slowly above 5 dpa. Most 300-series SSs exhibit strain softening, or dislocation channeling, and little or no uniform elongation at irradiation dose above 5 dpa.

The significance of material yield strength on IASCC susceptibility, particularly in the LWR environments, is discussed. Data on SCC susceptibility indicate that nonsensitized SSs with high tensile strength are susceptible to SCC in ultra-high purity water. The increases in yield strength can originate from surface or bulk cold work, weld shrinkage strain, and precipitation or irradiation hardening; all of these increase SCC susceptibility. At a given yield strength below 800 MPa, a similar crack growth behavior is observed for different grades of SSs, although the CGRs in low-potential water are up to an order of magnitude lower. However, at yield strengths of 800 MPa or higher, the CGRs in low- and high-potential environments are comparable.

Increased susceptibility to IASCC has often been attributed to the segregation of Si at the grain boundaries. Crack growth studies on CW SSs with 3-5 wt.% Si show unusually high CGRs, and the rates are insensitive to changes in applied K or corrosion potential of the environment. In contrast, SSRT test data on irradiated SSs with 0.5-1.8 wt.% Si show less irradiation hardening and greater elongation than steels containing 0.5 wt.% Si. Additional data are needed to establish the role of Si segregation on the IASCC susceptibility of irradiated SSs. Also, material SFE is an important parameter that determines the deformation mode. Alloys with low SFE, such as SSs with 8 wt.% Ni, deform entirely by planar slip. The role of the localized deformation mode on IASCC of austenitic SSs should be further investigated. The applicability of the fast reactor data to LWRs needs to be further investigated.

Correlations, developed by the MRP, are presented for estimating tensile yield and ultimate strengths and uniform and total elongation of austenitic SSs as a function of neutron dose. The tensile properties reach saturation at 5-20 dpa and do not seem to change significantly at higher dose levels. However, the majority of the data have been obtained on materials irradiated in a fast reactor, while data on LWR-irradiated materials are limited, in particular, above 10 dpa. The available data indicate that the yield and ultimate strengths of the LWR-irradiated materials are typically higher, and uniform and total elongations are lower than those of materials irradiated in fast reactors. These differences are most likely due to minor differences in material microchemistry and microstructure. For example, Cr depletion and Si and Ni enrichment are less in fast reactor irradiated materials. Also, the presence of He bubbles and cavities in materials irradiated to high dose levels in LWRs may be important for IASCC susceptibility of austenitic SSs.

Crack growth rate data on irradiated wrought and cast austenitic SSs as well as SS weld metal and weld HAZ materials in LWR environments have been compiled and evaluated to define threshold fluence for IASCC and to develop disposition curves for cyclic and IASCC growth rates for reactor core internal materials. As a result of complexities and uncertainties in experimental measurements, the SCC crack growth rate data in LWR environments show significant variability, and specific effects of these parameters on growth rates cannot be accurately determined under all conditions of interest. The importance of test procedures that closely reproduce the loading and environment conditions for reactor core internal components is discussed.

The results indicate that in the NWC BWR environment, neutron irradiation up to 0.45 dpa ( $3 \times 10^{20}$  n/cm<sup>2</sup>) has no effect on CGRs; the rates are below the NUREG-0313 disposition curve for nonirradiated materials in high-purity water containing 8 ppm DO. The CGRs for materials irradiated to higher neutron dose levels can be up to a factor of 40 higher. The CGRs for some SSs irradiated to 5-8 dpa (corresponding to a 60-year end-of-life neutron dose for BWRs) are a factor of 20 higher than the NUREG-0313 curve and 2-3 higher than the EPRI disposition curve for BWR core internal components. The CGR data for highly irradiated materials show unusual behavior. The SCC growth rates, in an NWC BWR environment, for SSs irradiated to 18 or 37.5 dpa are below the NUREG-0313 disposition curve for

nonirradiated SSs. The reason for the low CGRs observed for these materials in the high-potential BWR environment is not clear. Both of these high dose materials were from a decommissioned PWR.

The SCC growth rates in the HWC BWR environment show a significant decrease relative to those in the NWC BWR environment for SSs irradiated to less than 3 dpa; little or no reduction for some SSs irradiated to dose levels as low as 3-4 dpa, at least at stress intensity factor (K) values above 18 MPa m<sup>1/2</sup>; and no decrease for all SSs irradiated to 12-14.5 dpa. The CGRs for some of the materials irradiated to 3-4 dpa are above the CGR disposition curve proposed by EPRI for the HWC BWR environment. However, some tests that did not show the benefit of reduced corrosion potential on growth rates are often screened out because their loading conditions marginally exceeded the proposed K/size criterion based on an effective yield stress. On the other hand, several investigations on the validity of the proposed K/size criterion do not support a criterion based on an effective yield stress instead of the measured yield stress. Additional CGR data on SSs irradiated to 3-8 dpa are needed to accurately establish the threshold for IASCC susceptibility in low-potential environments.

The SCC growth rates in the PWR environment show significant variability. The CGRs for the same material and irradiation condition increase with increasing test temperature. The temperature dependence of growth rates may be represented by an activation energy of 100 kJ/mol. In PWR water at 320°C, most of the CGR data for SSs irradiated to 3 dpa are up to a factor of 5 above the NUREG-0313 curve for nonirradiated materials, and those for SSs irradiated to 11-25 dpa are nearly two orders of magnitude above the same curve. Also, as observed earlier for HWC BWR water, the CGRs in the PWR environment of SSs irradiated to 18 or 37.5 dpa are below the NUREG-0313 curve for nonirradiated SSs. The reason for the high CGRs for some SSs irradiated to 11.4 dpa and unusually low growth rates in SSs irradiated to 18 or 37.5 dpa is not known. Additional data on PWR materials irradiated at different temperatures (e.g., between 300 and 350°C) are needed to better understand the IASCC susceptibility of austenitic SSs in PWR environments.

All wrought and cast austenitic SSs and their welds, irradiated below a threshold neutron fluence are considered not susceptible to IASCC in a PWR environment. Based on laboratory SSRT data and PWR operating experience, a threshold fluence of  $2 \times 10^{21}$  n/cm<sup>2</sup> (3 dpa) has been proposed. For materials irradiated above this threshold, IASCC initiation data have been used to define for a given neutron dose, an apparent stress threshold below which IASCC initiation will not occur in a PWR environment. The existing IASCC initiation data have been reviewed to evaluate the adequacy of the database for developing screening criteria for the IASCC susceptibility of PWR core internal components. Most of the IASCC data have been obtained on CW Type 316 SS, while data on solution-annealed Type 304, 304L, or 316 SS are limited. Also, there are no data on cast austenitic SSs, SS welds, and weld HAZ materials. Several studies indicate that materials irradiated in fast reactors show lower susceptibility to IASCC than those irradiated in LWRs. The current IASCC initiation database, however, includes some tests on austenitic SS irradiated in the BOR-60 fast reactor.

Also, although a threshold fluence of 3 dpa has been defined for IASCC in the PWR environment, no IASCC initiation data are available on austenitic SSs irradiated between 3 and 9.5 dpa. Furthermore, nearly all of the high fluence (>20 dpa) data and the majority of the low fluence data are for materials irradiated below 325°C and, therefore, do not include the potential effects of additional precipitate phases, voids/cavities, and He generation rate on IASCC. In reactor core internal components, IASCC is likely to occur under creviced conditions. Nearly all of the IASCC initiation tests have been conducted in the normal PWR environment.

Limited fatigue CGR data in air on austenitic SSs irradiated to 2 dpa under LWR irradiation conditions indicate little or no effect of neutron irradiation on growth rates. Additional results on SSs irradiated in fast reactors at 427°C show only slightly higher CGRs (up to a factor of two higher) at low  $\Delta K$  values (less than 44 MPa m<sup>1/2</sup>). Also, tests on Type 304 and 316 SS irradiated in a thermal reactor at 288°C to 2.7 dpa and tested at 427°C showed superior resistance to crack growth; crack growth rates were 25 to 50% lower than those for nonirradiated materials.

In the NWC BWR environment, the cyclic CGRs of SSs irradiated to 0.45 dpa ( $3 \times 10^{20}$  n/cm<sup>2</sup>) are the same as those for nonirradiated materials, whereas the CGRs of SSs irradiated to 0.75-3.0 dpa are higher. The cyclic CGRs at low frequencies are decreased by more than an order of magnitude when the DO level is decreased by changing from NWC to HWC. A superposition model has been used to represent the cyclic CGRs of austenitic SSs. The CGR in the reactor environment is expressed as the superposition of the rate in air (mechanical fatigue) and the rates due to corrosion fatigue and SCC. The superposition model generally provides the best estimate, or slightly conservative estimates, of fatigue CGRs in NWC and HWC BWR environments.

Fatigue CGR data on austenitic SSs irradiated to higher neutron dose levels in the BWR environment or on irradiated austenitic SSs in the PWR environment are not available. Additional fatigue crack growth data under these material and environmental conditions are needed to develop fatigue CGR correlations for BWR and PWR core internal components.

## ACKNOWLEDGMENTS

The authors thank Torill Karlsen, OECD Halden Reactor Project, Halden, Norway; Anders Jensen, Studsvik Nuclear AB, Sweden; and Raj Pathania, Electric Power Research Institute, for providing the experimental data and for their helpful comments. The authors are grateful to Bill Shack for his invaluable input and guidance in preparing this report. This work is sponsored by the Office of Nuclear Regulatory Research, U.S. Nuclear Regulatory Commission, under Job Code N6818; Program Manager: Appajosula S. Rao.

## REFERENCES

1. S. M. Bruemmer, et al., EPRI TR-107159, Electric Power Research Institute, Palo Alto, CA, 1996.
2. P. Scott, J. Nucl. Mater. 211 (1994) 101-122.
3. P. L. Andresen, F. P. Ford, S. M. Murphy, and J. M. Perks, in: Proc. 4th Intl. Symp. on Environmental Degradation of Materials in Nuclear Power Systems -- Water Reactors, NACE, Houston, TX, 1990, pp. 1.83-1.121.
4. G. S. Was and P. L. Andresen, Corrosion Vol. 63, NACE, Houston TX, 2007, Paper No. 1.
5. K. S. Brown, and G. M. Gordon, in: Proc. Third Intl. Symp. on Environmental Degradation of Materials in Nuclear Power Systems -- Water Reactor, Metallurgical Society, Warrendale, PA, 1987, pp. 243-248.
6. G. M. Gordon and K. S. Brown, in: Daniel Cubicciotti, ed., Proc. 4th Intl. Symp. on Environmental Degradation of Materials in Nuclear Power Systems -- Water Reactor, NACE, Houston, TX, 1990, pp. 14.46-14.61.

7. F. Garzarolli, D. Alter, and P. Dewes, in: Proc. Intl. Symp. on Environmental Degradation of Materials in Nuclear Power Systems -- Water Reactor, American Nuclear Society, Lagrange, IL, 1986, pp. 131-138.
8. M. Kodama, et al., in: R. E. Gold and E. P. Simonen, eds., Proc. Sixth Intl. Symp. on Environmental Degradation of Materials in Nuclear Power Systems -- Water Reactor, Minerals, Metals & Materials Society, Warrendale, PA, 1993, pp. 583-588.
9. M. Kodama, et al., in: Proc. Fifth Intl. Symp. on Environmental Degradation of Materials in Nuclear Power Systems -- Water Reactor, American Nuclear Society, Lagrange, IL, 1991, pp. 948-954.
10. W. L. Clark and A. J. Jacobs, in: Proc. First Intl. Symp. on Environmental Degradation of Materials in Nuclear Power Systems -- Water Reactor, NACE, Houston, TX, 1983, p. 451.
11. A. J. Jacobs, G. P. Wozadlo, K. Nakata, T. Yoshida, and I. Masaoka, in: Proc. Third Intl. Symp. on Environmental Degradation of Materials in Nuclear Power Systems -- Water Reactor, Metallurgical Society, Warrendale, PA, 1987, pp. 673-681.
12. H. M. Chung and W. J. Shack, NUREG/CR-6892, ANL-04/10, 2006.
13. Andresen, P. L., Corrosion/02, NACE, Houston, TX, 2002, Paper No. 02509.
14. P. L. Andresen and F. P. Ford, Corrosion/95, NACE, Houston TX, 1995, Paper No. 419.
15. R. Stoenescu, M. L. Castano, S. van Dyck, A. Roth, B. van der Schaaf, C. Ohms, and D. Gavillet, in: T. R. Allen, P. J. King, and L. Nelson, eds., Proc. 12th Intl. Conf. on Environmental Degradation of Materials in Nuclear Power System -- Water Reactors, Minerals, Metals, & Materials Society, Warrendale, PA, 2005, pp. 267-275.
16. A. Jenssen, and L. G. Ljungberg, in: G. Airey et al., eds., Proc. Seventh Intl. Symp. on Environmental Degradation of Materials in Nuclear Power Systems -- Water Reactor, NACE, Houston, TX, 1995, pp. 1043-1052.
17. A. Jenssen and L. G. Ljungberg, in: R. E. Gold and E. P. Simonen, eds., Proc. Sixth Intl. Symp. on Environmental Degradation of Materials in Nuclear Power Systems -- Water Reactor, Minerals, Metals & Materials Society, Warrendale, PA, 1993, pp. 547-553.
18. F. P. Ford and P. L. Andresen, in: P. Marcus and J. Ouder, eds., Corrosion Mechanisms, Marcel Dekker, New York, 1994, pp. 501-546.
19. P. L. Andresen, In: Proc. Research Topical Symposium on Environmental Cracking, Corrosion/07, NACE, Houston, TX, 2007.
20. P. L. Andresen and M. M. Morra, in: T. R. Allen, P. J. King, and L. Nelson, eds., Proc. 13th Intl. Conf. on Environmental Degradation of Materials in Nuclear Power Systems -- Water Reactors, Canadian Nuclear Society, Toronto, Canada, 2007, Paper No. P0124.
21. S. M. Bruemmer, E. P. Simonen, P. M. Scott, P. L. Andresen, G. S. Was, and J. L. Nelson, J. Nucl. Mater. 274 (1999) 299-314.

22. P. J. Maziasz, *J. Nucl. Mater.* 205 (1993) 118-145.
23. S. J. Zinkle, P. J. Maziasz, and R. E. Stoller, *J. Nucl. Mater.* 206 (1993) 266-286.
24. D. J. Edwards, E. P. Simonen, and S. M. Bruemmer, *J. Nucl. Mater.* 317 (2003) 13-31.
25. S. M. Bruemmer, D. J. Edwards, B. W. Arey, and L. A. Charlot, in: *Proc. Ninth Intl. Symp. on Environmental Degradation of Materials in Nuclear Power Systems -- Water Reactor*, Metallurgical Society, Warrendale, PA, 1999, pp. 1079-1087.
26. S. M. Bruemmer, in: *Proc. Tenth Intl. Symp. on Environmental Degradation of Materials in Nuclear Power Systems -- Water Reactor*, NACE, Houston, TX, 2001, Paper No. 0008V.
27. G. E. Lucas, *J. Nucl. Mater.* 206 (1993) 287-305.
28. J. C. Van Duysen, P. Todeschini, and G. Zacharie, in: *16<sup>th</sup> International Symposium on Effects of Radiation on Materials*, American Society for Testing and Materials, ASTM STP 1175, 1993, pp. 747-776.
29. W. S. Hazelton and W. H. Koo, NUREG-0313, Rev. 2, 1988.
30. O. K. Chopra, B. Alexandreanu, E. E. Gruber, R. S. Daum, and W. J. Shack, NUREG/CR-6891, ANL-04/20, 2006.
31. O. K. Chopra, and W. J. Shack, NUREG/CR-6960, ANL-06/58, March 2008.
32. S. Ooki, Y. Tanaka, K. Takamori, S. Suzuki, S. Tanaka, Y. Saito, T. Nakamura, T. Kato, K. Chatani, and M. Kodama, in: T. R. Allen, P. J. King, and L. Nelson, eds *Proc. 12th Intl. Conf. on Environmental Degradation of Materials in Nuclear Power Systems - Water Reactors*, Minerals, Metals & Materials Society, Warrendale, PA, 2005, pp. 365-376.
33. P. L. Andresen and M. M. Morra, in: T. R. Allen, P. J. King, and L. Nelson, eds., *Proc. 12th Intl. Conf. on Environmental Degradation of Materials in Nuclear Power System -- Water Reactors*, Minerals, Metals, & Materials Society, Warrendale, PA, 2005, pp. 87-106.
34. D. Edwards, E. Simonen, S. Bruemmer, and P. Efsing, in: T. R. Allen, P. J. King, and L. Nelson, eds., *Proc. 12th Intl. Conf. on Environmental Degradation of Materials in Nuclear Power System -- Water Reactors*, Minerals, Metals, & Materials Society, Warrendale, PA, 2005, pp. 419-428.
35. D. Edwards, E. Simonen, and S. Bruemmer, in: T. R. Allen, P. J. King, and L. Nelson, eds., *Proc. 13th Intl. Conf. on Environmental Degradation of Materials in Nuclear Power Systems -- Water Reactors*, Canadian Nuclear Society, Toronto, Canada, 2007, Paper No. P0139.
36. *Materials Reliability Program A Review of Radiation Embrittlement for Stainless Steels (MRP-79)*, Rev. 1, EPRI Report 1008204, Sept. 2004.
37. A. Demma, R. Carter, A. Jenssen, T. Torimaru, and R. Gamble, in: T. R. Allen, P. J. King, and L. Nelson, eds., *Proc. 13th Intl. Conf. on Environmental Degradation of Materials in Nuclear Power Systems -- Water Reactors*, Canadian Nuclear Society, Toronto, Canada, 2007, Paper No. 114.

38. T. M. Karlsen, M. Espeland, and A. Horvath, HWR-773, OECD Halden Reactor Project, May 2005.
39. J. Conermann, R. Shogan, K. Fujimoto, T. Yonezawa, and T. Yamaguchi, in: T. R. Allen, P. J. King, and L. Nelson, eds., Proc. 12th Intl. Conf. on Environmental Degradation of Materials in Nuclear Power Systems -- Water Reactors, Minerals, Metals & Materials Society, Warrendale, PA, 2005, pp. 277-284.
40. K. Takakura, K. Nakata, M. Ando, K. Fujimoto, and E. Wachi, in: T. R. Allen, P. J. King, and L. Nelson, eds., Proc. 13th Intl. Conf. on Environmental Degradation of Materials in Nuclear Power Systems -- Water Reactors, Canadian Nuclear Society, Toronto, Canada, 2007, Paper No. P0009.
41. Materials Reliability Program Development of Material Constitutive Model for Irradiated Austenitic Stainless Steels (MRP-135), EPRI Report 1011127, Dec. 2004.
42. A. Jenssen, K. Gott, P. Efsing, and P. O. Andersson, in: Proc. 11th Intl. Symp. on Environmental Degradation of Materials in Nuclear Power Systems -- Water Reactors, American Nuclear Society, Lagrange, IL, 20, pp. 1015-102403.
43. T. Nakamura, M. Koshiishi, T. Torimaru, Y. Kitsunai, K. Takakura, K. Nagata, M. Ando, Y. Ishiyama, and A. Jenssen, in: T. R. Allen, P. J. King, and L. Nelson, eds., Proc. 13th Intl. Conf. on Environmental Degradation of Materials in Nuclear Power Systems -- Water Reactors, Canadian Nuclear Society, Toronto, Canada, 2007, Paper No. P0030.
44. R. Sumiya, S. Tanaka, K. Nakata, K. Takakura, M. Ando, T. Torimaru, and Y. Kitsunai, in: T. R. Allen, P. J. King, and L. Nelson, eds., Proc. 13th Intl. Conf. on Environmental Degradation of Materials in Nuclear Power Systems -- Water Reactors, Canadian Nuclear Society, Toronto, Canada, 2007, Paper No. P0072.
45. P. L. Andresen and M. M. Morra, Trans. ASME 129 (2007) 488-506.
46. R. Pathania, R. Carter, R. Horn, and P. Andresen, in: Proc. 14th Intl. Conf. on Environmental Degradation of Materials in Nuclear Power Systems -- Water Reactors, American Nuclear Society, Lagrange Park, IL, Paper No. 203178, 2009.
47. T. M. Karlsen and A. Horvath, HWR-770, OECD Halden Reactor Project, Dec. 2004.
48. J. Nakano, T. M. Karlsen, and M. Espeland, HWR-862, OECD Halden Reactor Project, Feb. 2007.
49. T. M. Karlsen, P. Bennett, and N. W. Hogberg, in: T. R. Allen, P. J. King, and L. Nelson, eds., Proc. 12th Intl. Conf. on Environmental Degradation of Materials in Nuclear Power Systems -- Water Reactors, Minerals, Metals & Materials Society, Warrendale, PA, 2005, pp. 337-348.
50. A. Jenssen, J. Stjarnsater, and R. Pathania, in: Proc. 14th Intl. Conf. on Environmental Degradation of Materials in Nuclear Power Systems -- Water Reactors, American Nuclear Society, Lagrange Park, IL, 2009.
51. O. K. Chopra, E. E. Gruber, and W. J. Shack, NUREG/CR-6826, ANL-03/22, 2003.

52. O. K. Chopra, B. Alexandreanu, E. E. Gruber, and W. J. Shack, in: T. R. Allen, P. J. King, and L. Nelson, eds., Proc. 12th Intl. Conf. on Environmental Degradation of Materials in Nuclear Power Systems -- Water Reactors, Minerals, Metals & Materials Society, Warrendale, PA, 2005, pp. 289-298.
53. J. Nakano, T. M. Karlsen, and M. Espeland, HWR-843, OECD Halden Reactor Project, Aug. 2008.
54. R. B. Davis and P. Andresen, Cooperative IASCC Research (CIR) Final Report, EPRI 1007378, Oct. 2002.
55. L. A. James and D. P. Jones, in: R. Rungta, ed., Proc. Conf. on Predictive Capabilities in Environmentally-Assisted Cracking, PVP Vol. 99, American Society of Mechanical Engineers, New York, pp. 363-414, 1985.
56. W. J. Shack and T. F. Kassner, NUREG/CR-6176, ANL-94/1, 1994.
57. P. Shahinian, H. E. Watson, and H. H. Smith, NRL Report 7446, Naval Research Laboratory, Washington, DC, July 1972.
58. P. Shahinian, in: C. J. Baroch, ed., Properties of Reactor Structural Alloys After Neutron or Particle Irradiation, ASTM STP 570, American Society for Testing and Materials, Philadelphia, PA, 1975, pp. 191-204.
59. L. A. James and R. L. Knecht, Nucl. Technol. 19 (1973) 148-155.
60. L. A. James, J. Nucl. Mater. 59 (1976) 183-191.
61. Shahinian, P., H. E. Watson, and H. H. Smith, "Neutron Irradiation Effects on Fatigue Crack Growth in Types 304 and 316 Stainless Steels," in Irradiation Effects on Reactor Structural Materials, Quarterly Progress Report 1 May – 31 July 1972, NRL Memorandum Report 2505, Naval Research Laboratory, Washington, DC, pp. 13-22, Aug. 1972.
62. Materials Reliability Program: PWR Internals Material Aging Degradation Mechanism Screening, and Threshold Values (MRP-175), EPRI Report 1012081, Dec. 2005.
63. R. P. Shogan, and T. R. Mager, in: Proc. 10th Intl. Conf. on Environmental Degradation of Materials in Nuclear Power Systems -- Water Reactors, NACE/ANS/TMS, Lake Tahoe, NV, Aug. 5-9, 2001, Paper No. 0030.
64. P. D. Freyer, T. R. Mager, and M. A. Burke, in: T. R. Allen, P. J. King, and L. Nelson, eds., Proc. 13th Intl. Conf. on Environmental Degradation of Materials in Nuclear Power Systems -- Water Reactors, Canadian Nuclear Society, Toronto, Canada, 2007, Paper No. P0034.
65. H. Nishioka, K. Fukuya, K. Fujii, and T. Torimaru, in: T. R. Allen, P. J. King, and L. Nelson, eds., Proc. 13th Intl. Conf. on Environmental Degradation of Materials in Nuclear Power Systems -- Water Reactors, Canadian Nuclear Society, Toronto, Canada, 2007, Paper No. P0040.
66. S. Fyfe, H. Xu, P. Scott, L. Fournier, and A. Demma, in: Proc. 14<sup>th</sup> Intl. Conf. on Environmental Degradation of Materials in Nuclear Power Systems -- Water Reactors, American Nuclear Society, Lagrange Park, IL, 2009.